# DEVELOPMENT OF NONDESTRUCTIVE TESTING TECHNIQUES FOR DETECTING STRESS IN FERROMAGNETIC MATERIALS

C. G. Gardner, et al

Southwest Research Institute

Prepared for:

Naval Air Development Center
Advanced Research Projects Agency

30 September 1971

# DEVELOPMENT OF NONDESTRUCTIVE TESTING TECHNIQUES FOR DETECTING STRESS IN FERROMAGNETIC MATERIALS

by
C. G. Gardner
G. A. Matzkanin
J. Lankford

**PHASE III**
**FINAL REPORT**
**SwRI Project No. 15-2474**
**Contract No. N00156-69-C-0856**

**Prepared for**
**Naval Air Engineering Center**
**Philadelphia, Pennsylvania**

**Sponsored by**
**Advanced Research Projects Agency**
**ARPA Order No. 1247, Amendment No. 1, Program Code No. 9D10**

**30 September 1971**



SOUTHWEST RESEARCH INSTITUTE
SAN ANTONIO HOUSTON

SOUTHWEST RESEARCH INSTITUTE
Post Office Drawer 28510, 8500 Culebra Road
San Antonio, Texas 78284

# DEVELOPMENT OF NONDESTRUCTIVE TESTING TECHNIQUES FOR DETECTING STRESS IN FERROMAGNETIC MATERIALS

by
C. G. Gardner
G. A. Matzkanin
J. Lankford

**PHASE III**
**FINAL REPORT**
**SwRI Project No. 15-2474**
**Contract No. N00156-69-C-0856**



Prepared for
**Naval Air Engineering Center**
**Philadelphia, Pennsylvania**

Sponsored by
Advanced Research Projects Agency
ARPA Order No. 1247, Amendment No. 1, Program Code No. 9D10

30 September 1971

Approved:
John R. Barton

John R. Barton, Director
Department of Instrumentation Research





56

## SUMMARY

The state of mechanical stress of a ferromagnetic material strongly influences its magnetic properties. In particular, characteristics of the abrupt, discontinuous, irreversible jumps in the magnetization (the Barkhausen effect) are stress sensitive. Instrumentation designed to detect and measure stress by generating Barkhausen jumps and inductively sensing them has proven to be a convenient and practical means of rapidly and nondestructively characterizing the state of stress of steels. To extend the capabilities of this stress measurement approach requires an improved understanding of the basic mechanisms by which stress affects Barkhausen jumps, and a clarification of the role played by factors other than stress. The overall objective of the present program was to investigate the fundamental aspects of the Barkhausen effect with the ultimate goal of more effectively exploiting this effect as a means of measuring applied and residual stresses in ferromagnetic materials.

Two experimental methods were employed in the investigation: (1) application of a multichannel pulse height analyzer to the study of certain statistical properties of the voltage pulses induced in a search coil by Barkhausen jumps; and (2) application of the Kerr magnetooptic effect to optically image magnetic domain structure and to study the effects of stress thereon by high-speed motion picture photography.

The investigation has resulted in the following major conclusions:

(1) Barkhausen jumps are actually of two types. One type involves comparatively large scale rearrangements of domain structure with 90° Bloch domain walls playing a prominent role; the other type results from abrupt movements of 180° Bloch domain walls whose motion is impeded by localized metallurgical inhomogeneities.

(2) A major mechanism by which stress influences the Barkhausen effect is suppression of the large scale domain rearrangements.

(3) The distribution of Barkhausen jumps along a branch of the technical hysteresis curve is altered in characteristic ways by stress.

(4) An increased density of dislocations, produced by plastic deformation, increases the incidence of Barkhausen jumps. This effect can to a significant extent be distinguished from the effect of stress by means of the distribution of jumps along the hysteresis curve.

(5) The pulse height analysis approach, which is digital rather than analog, has significant potential for further development as the basis for instrumentation for stress measurement and metallurgical characterization of ferromagnetic materials. This approach would complement the conventional analog signal processing approach.

TABLE OF CONTENTS


| | | Page |
|---|---|---|
| LIST OF ILLUSTRATIONS | | v |
| I. | INTRODUCTION | 1 |
| | 1.1 Program, Background and Objectives | 1 |
| | 1.2 Scope of Phase III | 3 |
| 2. | EXPERIMENTAL METHODS AND PROCEDURES | 5 |
| | 2.1 Inductive Coil | 5 |
| | 2.2 Magnetooptic Cinematography | 10 |
| 3. | EXPERIMENTAL RESULTS | 16 |
| | 3.1 Inductive Search Coil Pulse Height Analysis | 16 |
| | 3.1.1 Results for the Polycrystalline Specimen in the Elastic Strain Region | 19 |
| | 3.1.2 Results for Polycrystalline Specimens in the Plastic Strain Range | 19 |
| | 3.1.3 Results for the Single Crystal Specimen | 23 |
| | 3.2 Magnetooptic Cinematography | 31 |
| 4. | DISCUSSION OF RESULTS | 36 |
| 5. | CONCLUSIONS AND RECOMMENDATIONS | 40 |
| REFERENCES | | 42 |
| APPENDIX A - SHAPING OF BARKHAUSEN PULSES FOR MULTICHANNEL PULSE HEIGHT ANALYSIS | | |
| APPENDIX B - MAGNETOOPTIC PHOTOMETRY | | |
| APPENDIX C - LIST OF PUBLICATIONS AND PRESENTATIONS | | |

## LIST OF ILLUSTRATIONS


| Number | | Page |
|---|---|---|
| 1. | Diagram of Barkhausen Pulse Height Analysis System | 6 |
| 2. | Laboratory Arrangement for Studying the Barkhausen Effect | 7 |
| 3. | Barkhausen Pulses from Polycrystalline Fe-3.2%Si | 9 |
| 4. | Arrangement for Studying the Barkhausen Effect by Multiscaling | 11 |
| 5. | Multiscaling Barkhausen Pulse Distribution for Fe-3.2%Si | 11 |
| 6. | Diagram of Magnetooptic Cinematography System | 13 |
| 7. | High-Speed Magnetooptic Domain Cinematography System | 14 |
| 8. | Single Crystal Domain Structure at Various Stages of Magnetization Reversal | 15 |
| 9. | Barkhausen Pulse Height Distribution for Annealed Polycrystalline Fe-3.2%Si Specimen | 17 |
| 10. | Multiscaling Barkhausen Pulse Distribution for Annealed Polycrystalline Fe-3.2%Si Specimen | 20 |
| 11. | Total Barkhausen Count Number Versus Elastic Strain for Polycrystalline Fe-3.2%Si | 21 |
| 12. | Stress-Strain Curve for Polycrystalline Fe-3.2%Si Specimen | 22 |
| 13. | Total Barkhausen Pulses per Magnetization Reversal Versus Strain | 24 |
| 14. | Average Barkhausen Pulse Height Versus Strain | 25 |
| 15. | Variation of Average Pulse Height with Elastic Recovery and Reloading of a Plastically Deformed Specimen | 26 |

LIST OF ILLUSTRATIONS (Contd.)


| Number | | Page |
|---|---|---|
| 16. | Variation of Total Count Number with Elastic Recovery and Reloading of a Plastically Deformed Specimen | 27 |
| 17. | Multiscaling Barkhausen Pulse Distributions for Various Stress-Strain States | 28 |
| 18. | Dimensions and Crystallographic Orientation of Fe-3.1%Si Single Crystal | 29 |
| 19. | Orientation of Crystalline Axes Relative to Magnetooptic Viewing Plane | 29 |
| 20. | Barkhausen Pulse Height Distributions for Fe-3.1%Si Single Crystal | 30 |
| 21. | Multiscaling Barkhausen Pulse Distributions for Fe-3.1%Si Single Crystal | 32 |
| 22. | Overall Domain Structure of Demagnetized Fe-3.1% Single Crystal | 33 |
| 23. | Single Crystal Domain Structure at Various Stages of Magnetization Reversal | 34 |
| 24. | Analog Barkhausen Signals for Two components of Split Inner Ring Thrust Bearing | 37 |
| A1. | Pulse Shaping Effect of Strobed Pulse Stretcher | |
| A2. | Barkhausen Pulse Height Distribution | |
| B1. | Schematic of Dual Beam Magnetooptic Photometric Barkhausen Experiment | |

# I. INTRODUCTION

## 1.1 Program, Background and Objectives

The need for practical methods of nondestructively assessing the state of mechanical stress of critical metal components is well recognized. In particular, alternatives to the somewhat complicated and cumbersome method of X-ray diffraction are desirable. In the case of ferromagnetic materials, the stress dependence of magnetic properties has been considered as a candidate approach. To date, the most fruitful development along this line has been the exploitation of the stress dependence of the Barkhausen effect, i.e., abrupt, localized, irreversible rearrangements of magnetic domain structure[1]. Instrumentation based on this approach has currently reached a notable state of refinement, and is now beginning to be seriously considered as an alternative for X-ray diffraction in certain cases[2]. However, both the continued development and the application of this instrumentation has to an extent been impeded by inadequacies in fundamental understanding of the underlying phenomena. The manner in which composition, grain structure, defect state, internal stress state, geometry, etc., affect ferromagnetic properties is exceedingly complex and incompletely understood. The Barkhausen effect, in particular, though long known, has only recently begun to be studied by modern quantitative methods.

Present versions of practical instrumentation for detecting and characterizing the Barkhausen effect entail inductively coupling a search coil to a ferromagnetic specimen, either by surrounding the specimen with the search coil or by placing the search coil in proximity to the specimen[3]. The magnetization of the specimen is then cyclically reversed by applying an alternating external magnetic field, usually of maximum intensity sufficient to technically saturate the specimen. As the magnetization of the specimen varies, abrupt, localized changes in magnetization (Barkhausen "jumps") occur, producing rapid changes in the magnetic flux threading the search coil. These flux changes result in corresponding voltage pulses at the terminals of the search coil. If the search coil is connected to an appropriate amplifier, the resulting signal can be displayed on a cathode ray oscilloscope. The induced signal is found to consist of a sequence of voltage pulses of somewhat random amplitude, duration, and temporal separation. In terms of harmonic content, for a signal train corresponding to a full magnetization reversal, the signal may be roughly described as "noise" with frequency components of significant amplitude from approximately 1 KHz to several hundred KHz; above 100 KHz the amplitude of the signal is, however, practically negligible.

Various features of the Barkhausen signal have been demonstrated to be influenced by applied or residual mechanical stresses[4]. For example, the integrated power per magnetization reversal is such a feature. Other such features are the peak signal amplitude and the average signal amplitude. All these quantities may be conveniently measured by standard analog electronic methods, and this approach has been successfully made the basis for practical stress-measuring instrumentation. The empirical background pertaining to this approach has been described in References 4, 5 and 6. The work described in this report was conducted as part of a program the overall objective of which was to investigate the fundamental mechanisms involved in the Barkhausen effect, with the ultimate aim of more effectively exploiting this effect as a means of measuring applied and residual stresses in ferromagnetic materials, and otherwise nondestructively characterizing such materials.

In Phase I of the program, inductive studies of the Barkhausen effect were performed using a strictly analog approach. The frequency response of several search coil configurations was determined and the power spectral density found to be approximately proportional to $f^{-2}$, where f is the frequency. Stress-dependence studies confirmed a greater integrated total power for tension than for compression in a high-strength alloy steel. Analytical studies were carried out for typical non-encircling search coil geometries in an effort to interpret results theoretically.

The major part of the effort of Phase II was devoted to perfecting the apparatus and experimental technique required to perform photometric and cinematographic studies of dynamical magnetic domain processes as revealed by the longitudinal Kerr magnetooptic effect. The technical problems encountered in this aspect of the work proved to be somewhat more difficult than originally anticipated, and a correspondingly greater portion of the total technical effort was expended in solving them. However, the expended effort did result in a satisfactory solution of the problems encountered, with the result that high quality still and motion pictures of domains were obtained, analysis of which has clarified the fundamental role which the mechanical stress field plays in the Barkhausen effect. In addition to the magnetooptic effort, progress was made in using the inductive coil approach to study the Barkhausen effect. In particular, rod type specimens of polycrystalline silicon-iron suitable for use in the (previously designed and fabricated) nonmagnetic uniaxial stress fixture were designed and fabricated. Further, a bias field solenoid capable of accommodating these specimens and their corresponding search coils, and capable of being used with the specimens while they are in the stress fixture, was designed and fabricated. Preparations were made for the incorporation of a multichannel pulse height analyzer into the data acquisition system.

## 1.2 Scope of Phase III

Although present versions of practical Barkhausen stress measuring instrumentation make use of analog electronic methods for measuring various features of the Barkhausen signal, inquiries into the basic phenomena lead one to investigate in greater detail the characteristics of the direct unprocessed Barkhausen signal. One approach to this it to investigate the characteristics of the voltage pulses corresponding to individual Barkhausen jumps. If the rate of change of magnetization is sufficiently slow, and if circuitry of appropriate response time is used, most of the pulses of amplitude above some characteristic value occur in discreet, nonoverlapping fashion. Each pulse can then be characterized in terms of polarity, amplitude, duration, and "impulse", i.e., $\int V(t)dt$. The sequence of Barkhausen pulses corresponding to a given segment of the technical magnetization curve is not exactly reproducible from one magnetization cycle to another. Hence one must investigate the pulse characteristics in statistical terms. In Phase III of the investigation, two types of Barkhausen pulse distributions were singled out for study: these were (1) the number of pulses, sorted according to amplitude, occurring during a complete reversal of specimen magnetization, and (2) the total number of pulses, without regard to amplitude, occurring in successive increments of the applied field during a complete reversal of the magnetization. In other words, two important questions were broached: first, what is the relative frequency of occurrence of Barkhausen pulses of a given amplitude?; and second, what is the relative number of pulses occurring at successive points along the magnetization curve? These aspects were selected because visual examination of oscillographic records of Barkhausen pulse sequences suggested that it was probably these properties which lay behind the characteristic shapes of the analog signatures. Other aspects of the pulse distribution could, of course, be studied, but the present investigation was limited to the two aspects mentioned.

The material for the specimens used in this study was mild silicon iron. This material was chosen for these initial studies because of its comparatively simple and well-studied metallurgy, because many of its magnetic properties have already been studied, and because it could be conveniently prepared in both single-crystal and polycrystalline form.

Since it is desired ultimately to be able to interpret the results of inductive search coil detection of the Barkhausen effect in terms of the underlying processes involving magnetic domain rearrangements, it was decided that direct observations of such processes, particularly as they are influenced by stress, would greatly help in such interpretation. Accordingly, an experimental investigation of the influence of stress on

the magnetization of a single crystal specimen was undertaken using high-speed cinematography of the domain structure as optically imaged by the Kerr Magnetooptic effect[7]. Some results of this investigation will be discussed in relation to the inductive search coil findings.

The major effort in Phase III has been devoted to perfecting the digital inductive approach to the Barkhausen effect whereby a pulse height analyzer is used to study the Barkhausen voltage pulses induced in a search coil. By this method, the effects of elastic and plastic deformation were studied on the amplitude distribution of Barkhausen pulses and the number distribution of Barkhausen pulses along the magnetization curve in several specimens.

Besides the inductive search coil studies conducted during Phase III, a high repetition rate pulsed argon laser was acquired for high speed cinematographic studies of domain dynamics. After adequate development of the experimental technique, studies were made at framing rates of 5,000 pictures per second of the influence of applied compressive stress on the dynamic surface domain structure of a Fe-3.1%Si single crystal.

A list of publications and meeting and symposia presentations resulting from this program may be found in Appendix C.

## 2. EXPERIMENTAL METHODS AND PROCEDURES

### 2.1 Inductive Coil

The inductive method is based on a measurement of some characteristic of the voltage pulse induced by a Barkhausen jump in a search coil. It was shown by Tebble, Skidmore and Corner[8] that for the case of the search coil time constant much larger than the duration of the Barkhausen jump itself, the shape of the induced voltage pulse is determined largely by the time constants of the search coil circuit, the pulse amplitude being proportional to the total flux change accompanying the Barkhausen jump. This "ballistic method has been used in almost all recent quantitative investigations of the Barkhausen effect and was also the approach used in the inductive experiments performed in this program.

A block diagram of our experimental arrangement is shown in Figure 1 and a photograph of the laboratory setup is shown in Figure 2. As indicated in previous reports, specimen-encircling cylindrical geometry has been used throughout these experiments. This choice was made because of the suitability of this configuration for well-defined experimental conditions, and to facilitate interpretation in terms of existing theory. A brief description of the basic components constructed and used is given in Tables I, II and III.

The solenoid was energized by a programmable bipolar power supply; and a signal generator provided a low frequency triangular driving waveform. The bandwidth of the overall amplification system was ordinarily limited to 1-10 KHz. Typical oscilloscope traces of Barkhausen signals obtained with the apparatus are illustrated in Figure 3. The top photograph shows that the magnetizing field supplied by the solenoid was sufficient to achieve saturation, and clearly illustrates the Barkhausen noise pulses in comparison to the background noise apparent in the saturation region at the ends of the sweep. The bottom photograph shows resolved Barkhausen voltage pulses on an expanded time scale.

The multichannel pulse height analyzer shown in Figure 2 is of the type commonly used in nuclear pulse spectroscopy. It basically comprises an analog-to-digital converter, a 1024 storage location (channel) digital memory, logic circuitry, and memory display/output circuitry. In the pulse height analysis mode, the amplitude of an incoming pulse is digitized and measured; on a linearly calibrated scale, the memory channel to which the measured amplitude corresponds is incremented one "count". Thus a distribution of number-of-pulses versus pulse amplitude can be accumulated.

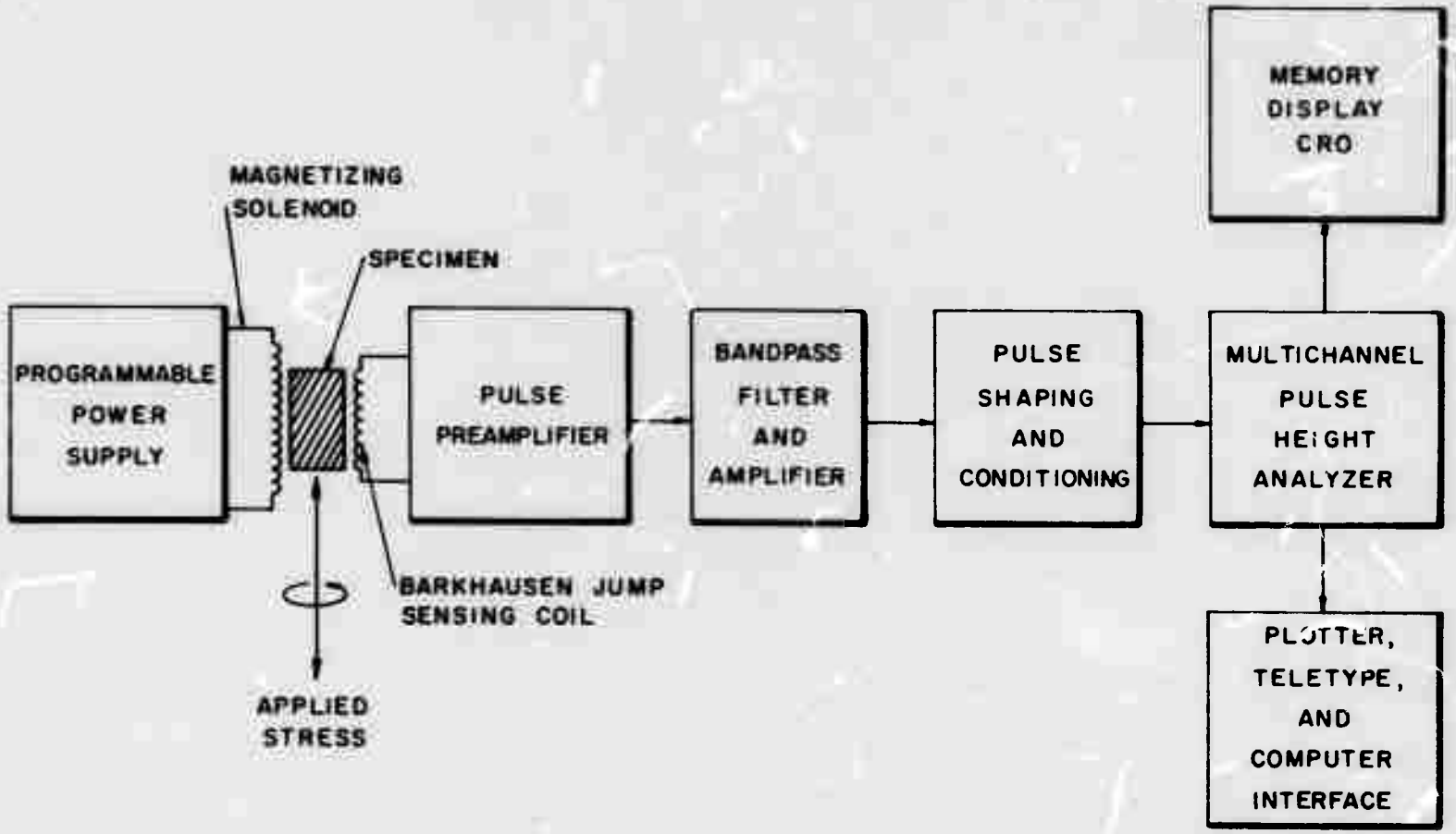


FIGURE 1. DIAGRAM OF BARKHAUSEN PULSE HEIGHT ANALYSIS SYSTEM

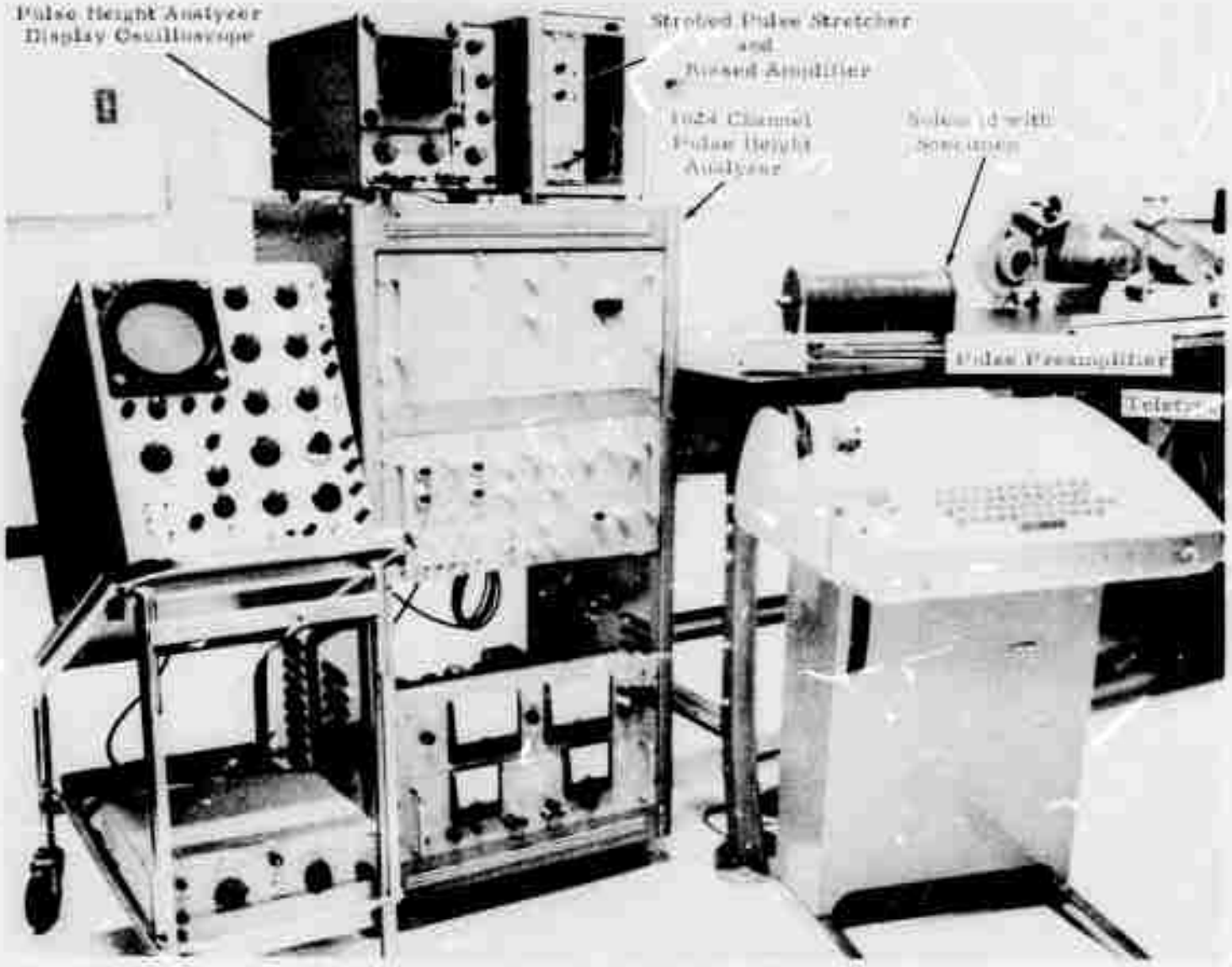


FIGURE 2. LABORATORY ARRANGEMENT FOR STUDYING THE BARKHAUSEN EFFECT.

## TABLE I

## SEARCH COIL PARAMETERS

| | |
|---|---|
| Length | 4 in. |
| ID | 0.710 in. |
| OD | 0.735 in. |
| Number of turns | 1268, #38 copper wire |
| DC resistance | 105 Ω |
| Series Inductance | 5 mh |
| Time Constant | 200 μs |

## TABLE II

## PREAMPLIFIER PARAMETERS

| | |
|---|---|
| Gain | 1000X |
| Bandwidth between 3 db points | 50 Hz to 200 KHz for a 100 Ω input impedance |
| Peak-to-Peak noise | 5 μv referred to the input |

## TABLE III

## SOLENOID PARAMETERS

| | |
|---|---|
| Bore | 1 in. |
| Length | 11 in. |
| Number of turns | 8100, #18 copper wire |
| Field | 380 Oe/amp |
| Maximum field used | 380 Oe |

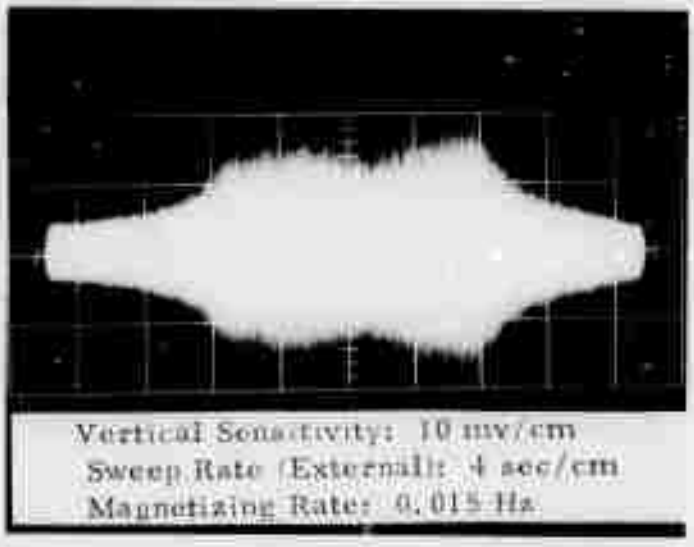


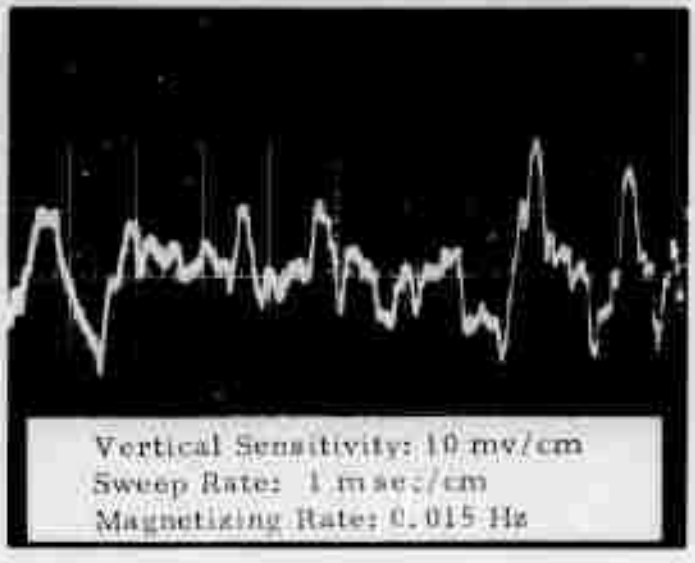


FIGURE 3. BARKHAUSEN PULSES FROM POLYCRYSTALLINE Fe-3.2%Si

An innovation in inductive coil methods devised in this program is the development of a procedure for obtaining distributions of the total number of Barkhausen jumps which occur per unit increment in the magnetic field applied to the specimen. The procedure involves use of the multiscaling mode of the pulse height analyzer in which only one memory channel is active at a given time, all incoming pulses, regardless of amplitude, being counted in that channel; each channel is consecutively activated for a certain "dwell time." The entire memory is scanned synchronous with one half-cycle of the alternating magnetic field applied to the specimen. Thus a "multiscaling distribution" is accumulated showing the number of Barkhausen pulses recorded in consecutive increments along the magnetization curve. The method is illustrated schematically in Figure 4. A trigger pulse from the magnetizing current signal generator is used to initiate multiscaling at the beginning of the current sweep so that the time scales of the multiscaling sweep and the magnetizing sweep can be synchronized. Since the multiscaling input of the analyzer requires pulses between 3 and 6 volts in amplitude whereas the Barkhausen pulses cover a much broader amplitude spectrum. The delayed trigger pulse mode of a Tektronix 545A oscilloscope was therefore used as a strobed pulse generator supplying constant amplitude pulses synchronous with the Barkhausen pulses. A representative example of a Number-vs-H distribution obtained by multiscaling is shown in Figure 5. This procedure enables one to determine the regions of the magnetization curve in which the largest number of Barkhausen jumps occur, without regard to their size.

In the performance of the inductive Barkhausen experiments, the data accumulated in the pulse height analyzer memory were subsequently recorded on a punched tape via an interfaced teletype terminal. The data were then processed using a specially developed computer program which provides either linear or semi-logarithmic plots and total count numbers between selected channels.

## 2.2 Magnetooptic Cinematography

The magnetooptic approach to the study of magnetization processes makes use of the Kerr effect whereby surface domains may be imaged by the effective polarization rotation which occurs when a linearly polarized light beam is reflected from a magnetized surface (see Phase II, Final Report for further details). Domain dynamics can therefore be studied cinematographically. However, a difficulty arises in that with respect to the incident polarization, the intensity of the emerging light is extremely low, the overall attenuation being on the order $10^{-6}$. Thus, for high speed cinematographic studies, a high power, fast repetition

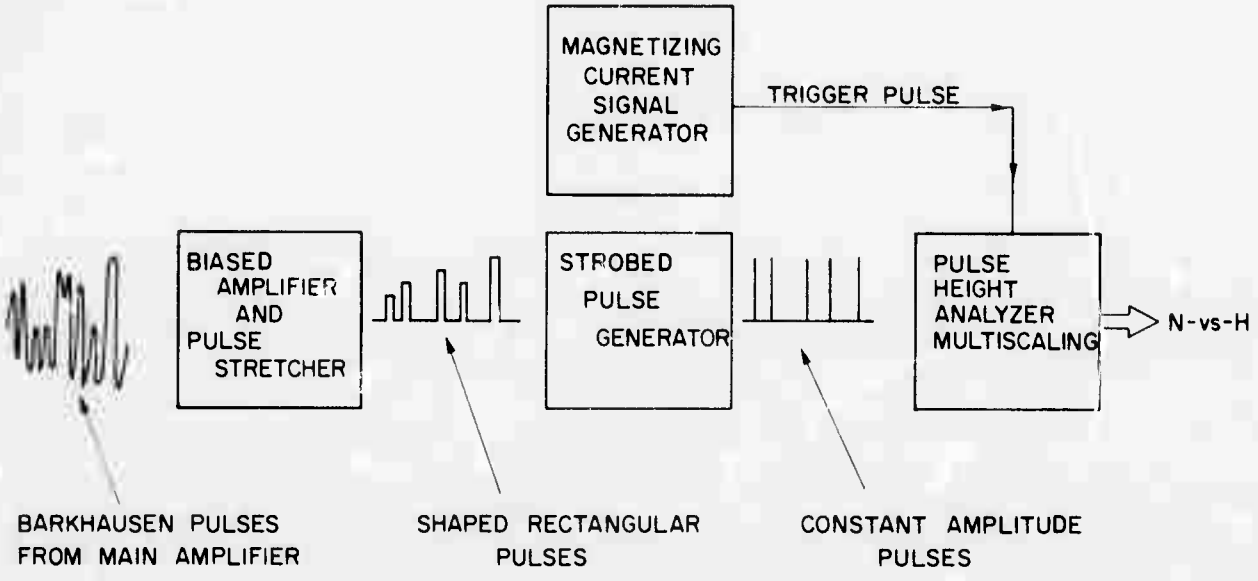


FIGURE 4. ARRANGEMENT FOR STUDYING THE BARKHAUSEN EFFECT BY MULTISCALING

FIGURE 5. MULTISCALING BARKHAUSEN PULSE DISTRIBUTION FOR Fe-3.2%Si

rate pulsed light source is required. A recently introduced stroboscopic argon ion laser was successfully adapted for this purpose. Figures 6 and 7 show respectively a schematic diagram and a photograph of our experimental arrangement. The laser normally emits a 16 $\mu$sec pulse with a peak power of 15 watts at a repetition rate of 600 pulses per second. However, for high-speed work, the laser can be operated in a "burst" mode in which the repetition rate may be increased to as high as 6000 pulses per second for periods up to two seconds. External triggering is used to synchronize the individual light pulses with the shutter openings of a high-speed movie camera. Since the flash synchronization pulses from the camera are not of a shape suitable for triggering the laser, it was found convenient to use the delayed trigger of a Tektronix 545A oscilloscope to provide appropriately shaped trigger pulses, and also to provide variable delay of the trigger pulses so that strobing between the laser pulses and the full shutter open condition of the camera can be readily achieved. After some initial work with ultra high-speed Kodak 2485 recording film, it was found that such high speed film is not necessary and that slower, finer grain Kodak 4X is adequate. Figure 8 shows a few representative frames from a 400 ft. roll of film made at a framing rate of 5000 pictures per second showing domains on the surface of a single crystal of Fe-3.1%Si.

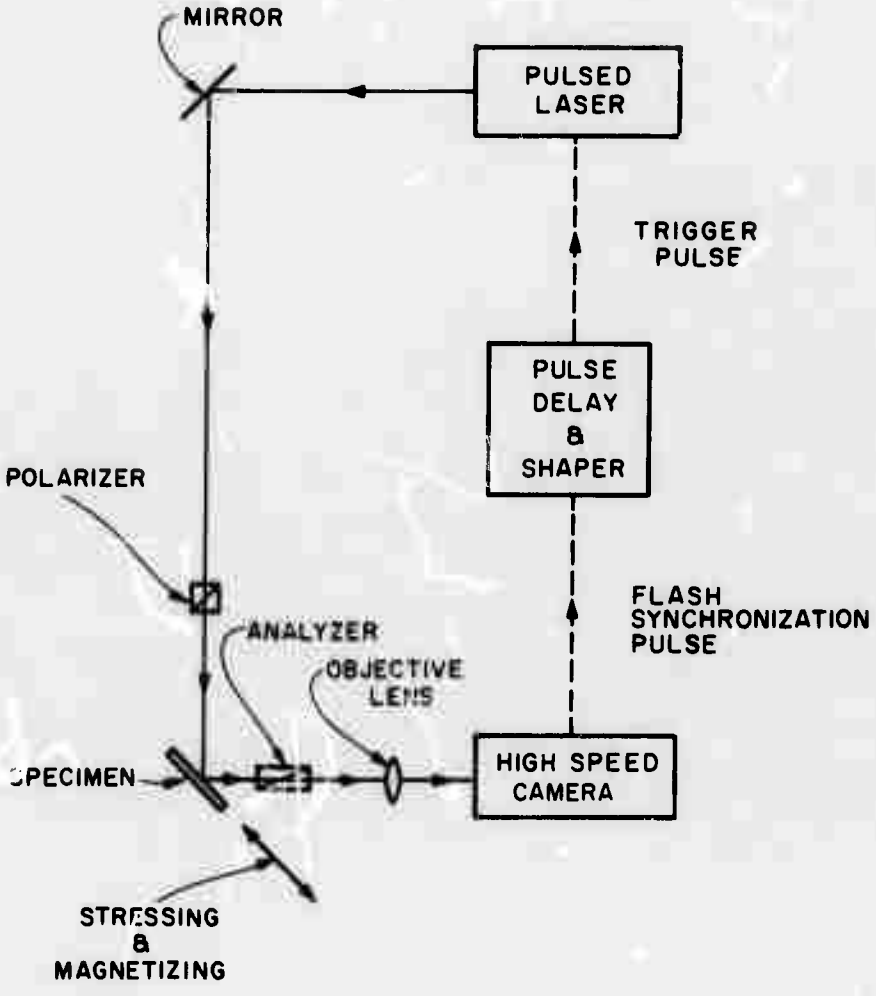


FIGURE 6. DIAGRAM OF MAGNETOOPTIC CINEMATOGRAPHY SYSTEM

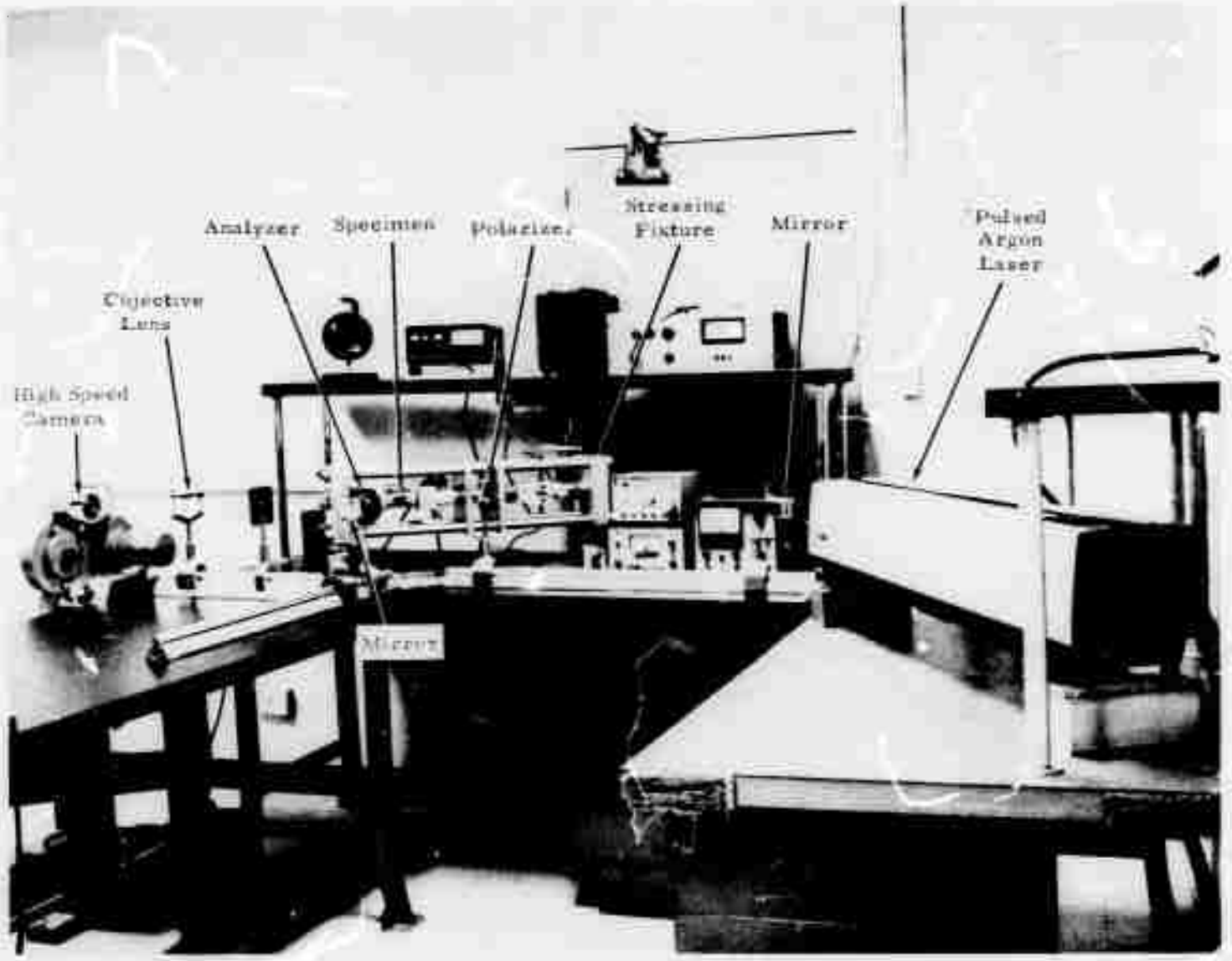


FIGURE 7. HIGH-SPEED MAGNETOOPTIC DOMAIN CINEMATOGRAPHY SYSTEM

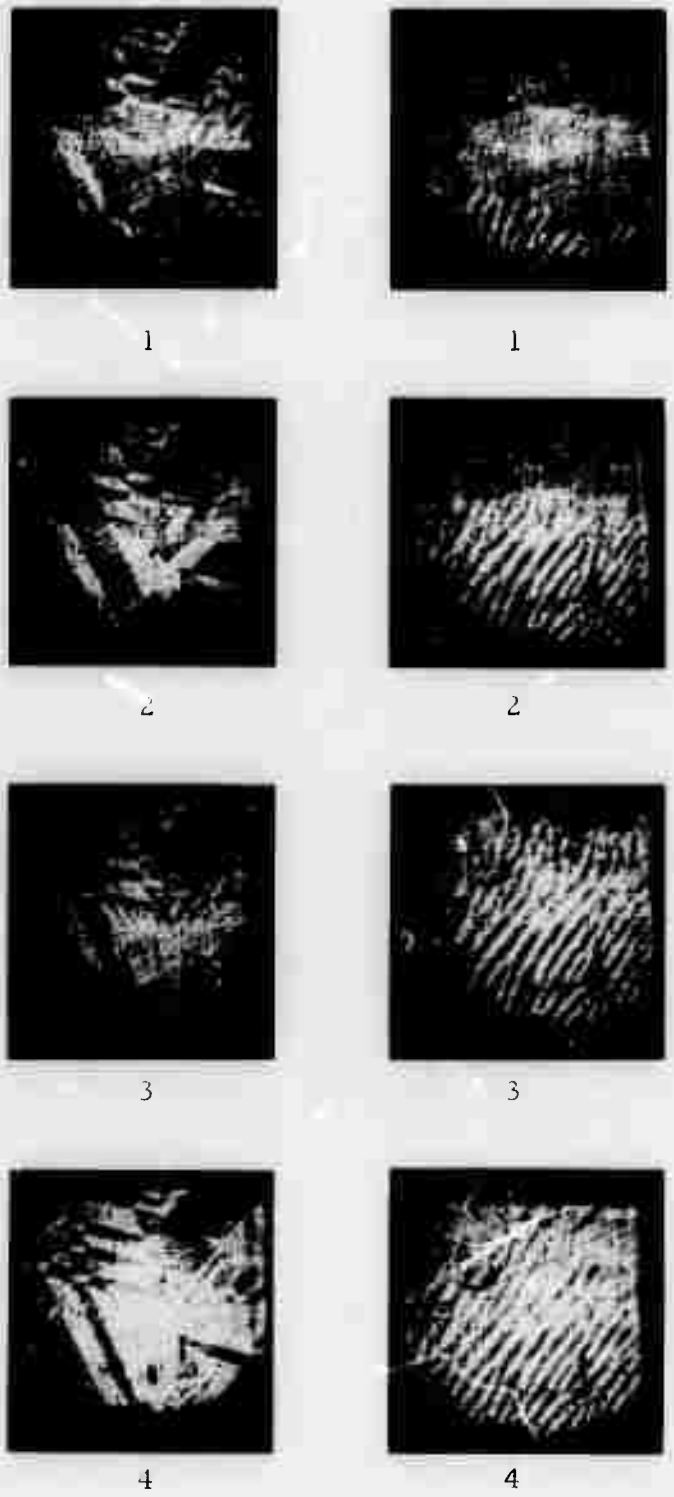


Original framing rate: 5000/sec

Interval between successive frames shown here: 1/20 sec

Magnification: 3X

a. Crystal Unstressed b. 6.6 kpsi Uniaxial Compression

FIGURE 8. SINGLE CRYSTAL DOMAIN STRUCTURE AT VARIOUS STAGES OF MAGNETIZATION REVERSAL

# 3. EXPERIMENTAL RESULTS

## 3.1 Inductive Search Coil Pulse Height Analysis

According to the procedures explained in the preceding Chapter, two types of Barkhausen pulse height analyses were carried out. In the first of these, called simply the pulse height distribution, all the pulses detected during a complete reversal of the magnetization of a specimen were fed to the pulse height analyzer which sorted the pulses according to their respective amplitudes, and stored in memory the number of pulses in each of 256 pulse amplitude increments. When plotted graphically, this data results in a histogram showing the number of pulses of a given amplitude versus the amplitude.

In the second type of pulse analysis, the ordinant of the distribution is proportional to the external field applied to the specimen during a complete reversal of the magnetization; this is divided into 256 increments. The ordinant is the number of recorded jumps (without regard to amplitude) occurring during a given increment of the applied field. The resultant graph thus shows the total intensity or rate of Barkhausen jumps as a function of the applied field, or, by using the hysteresis curve, as a function of the net magnetization of the specimen.

These two types of pulse distributions were obtained for polycrystalline silicon iron specimens subjected to tensile and compressive stresses in both elastic and plastic regions. They were also obtained for the silicon iron single crystal under an elastic compressive stress.

The pulse height distribution for the polycrystalline specimen in its initial (annealed) condition is shown in Figure 9. The distribution is plotted on a semilogarithmic scale. The distribution, thus plotted, is reasonably linear. Except in the region of small pulse amplitude, this linear character of the pulse height distribution was found for all stress-strain conditions of the specimens. Thus to a reasonable approximation, these distributions for the polycrystalline specimen may be represented by the empirical relation

$$N_m = N_o \exp(-Km\Delta) \qquad (1)$$

where

$N_m$ = number of pulses of amplitude m

$N_o$ = number of pulses of minimum amplitude

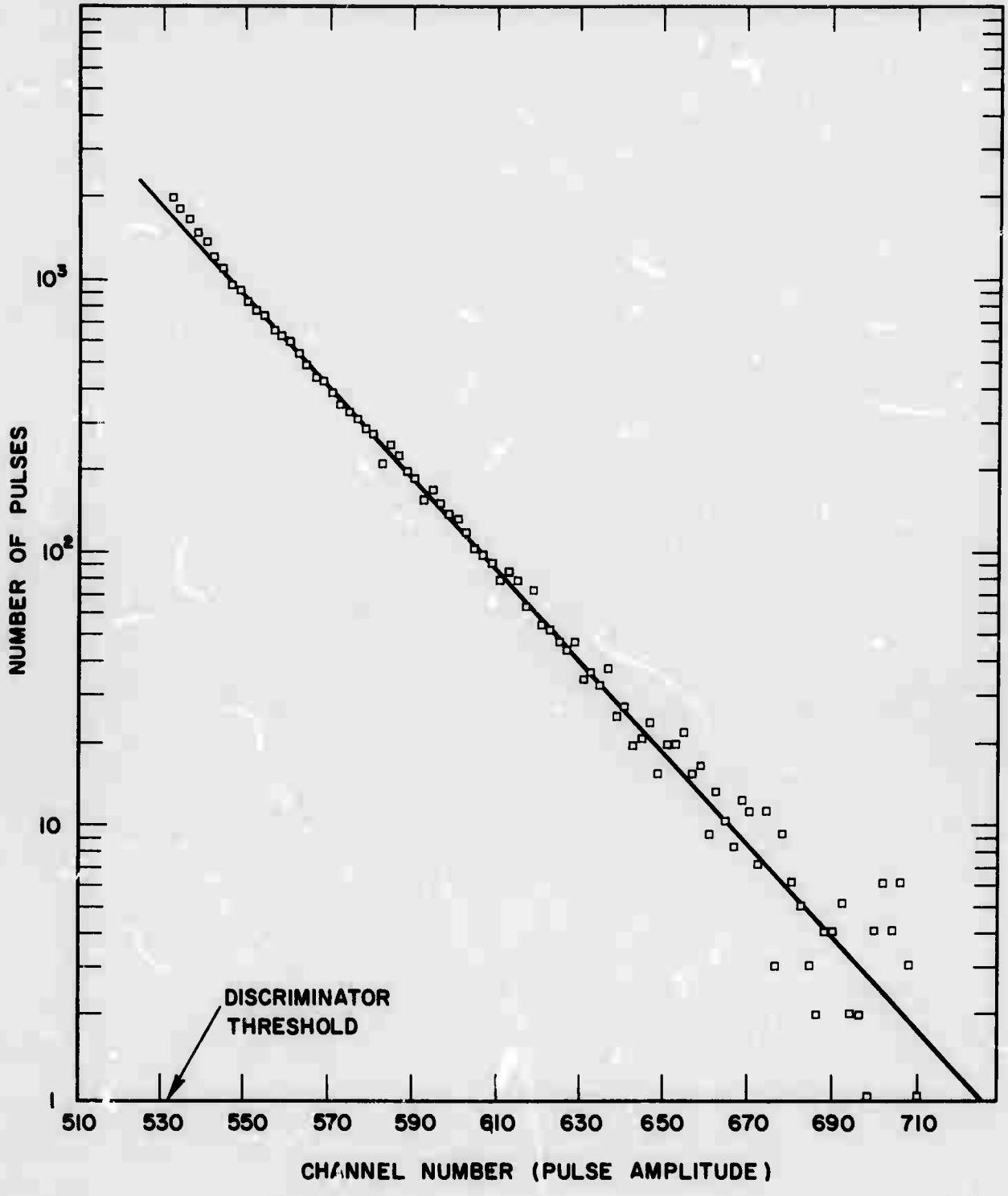


2300

FIGURE 9. BARKHAUSEN PULSE HEIGHT DISTRIBUTION FOR ANNEALED POLYCRYSTALLINE Fe-3.2%Si SPECIMEN

$K$ = an empirically determined positive constant

$\Delta$ = increment in pulse amplitude, per channel

$m$ = channel number (integer)

Here the amplitude is with respect to the particular lower level of pulse height discrimination used in the experiment, and not with respect to zero. For lower settings of the discriminator, electronic noise predominates.

The two parameters $N_o$ and K thus characterize the pulse height distribution. For interpretive purposes, it is useful to employ two additional parameters, namely, the total pulse number per magnetization reversal, $N_T$, and the average pulse amplitude, $\langle v \rangle$. The total pulse number is obtained simply by summing the number of counts in all channels. The average pulse amplitude may be computed from the formula

$$\langle v \rangle = \frac{\sum_{i=1}^{M} N_i V_i}{N_T} \tag{2}$$

$$= V_o + (\Delta) \frac{\sum_{i=1}^{M} i \cdot N_i}{N_T} \tag{3}$$

where

$N_i$ = number of counts in channel i

$V_i$ = pulse height (in volts) corresponding to channel i

$\Delta$ = pulse amplitude increment per channel

$V_o$ = pulse amplitude corresponding to channel zero.

$M$ = maximum channel number

Since $V_o$ and $\Delta$ remained the same throughout the experiment, the dimensionless quantity

$$\langle h \rangle \equiv \sum_{i=1}^{M} i \cdot N_i \quad / N_T \tag{4}$$

contains all the significant information so far as $\langle v \rangle$ is concerned; for simplicity the experimental results are presented in terms of $\langle h \rangle$. Thus the parameters $N_T$ and $\langle h \rangle$ may be expected to vary with the properties of the specimen and the external conditions affecting it.

The multiscaling pulse distribution for the initial condition of the same polycrystalline specimen is shown in Figure 10. Also shown in the figure is the branch of the smooth technical magnetization curve for a corresponding reversal of the magnetization of this specimen. The magnetization curve was obtained with a simple operational amplifier hysteresigraph. One notes that a peak occurs in the region of each of the "knees" of the magnetization curve, (identified as A and B in the figure), with a minimum (identified as C) in the region of the steep, central part of the magnetization curve.

### 3.1.1 Results for the Polycrystalline Specimen in the Elastic Strain Region

Figure 11 shows a graph of $N_T$, the total number of detected Barkhausen pulses per magnetization reversal, as a function of strain for uniaxial loading of a polycrystalline silicon iron specimen. The data shown were obtained from the multiscaling distributions for this specimen; the behavior of $N_T$ versus strain determined from the pulse height distribution was not significantly different from that determined from the multiscaling distribution. For this specimen, $N_T$ was not found to vary significantly with tensile strain in the elastic range; however, under compression $N_T$ increased monotonically with strain. The average pulse height parameter $\langle h \rangle$ (defined by Equation (4))was also determined as a function of strain for the same experimental conditions. However, no strong dependence of $\langle h \rangle$ upon strain in the plastic range was observed.

### 3.1.2 Results for Polycrystalline Specimens in the Plastic Strain Range

After its initial characterization, the polycrystalline specimen was pulled in tension. Figure 12 shows the stress-strain history; points on this curve at which pulse height and multiscaling distributions were obtained are indicated on the figure by numbered arrows.

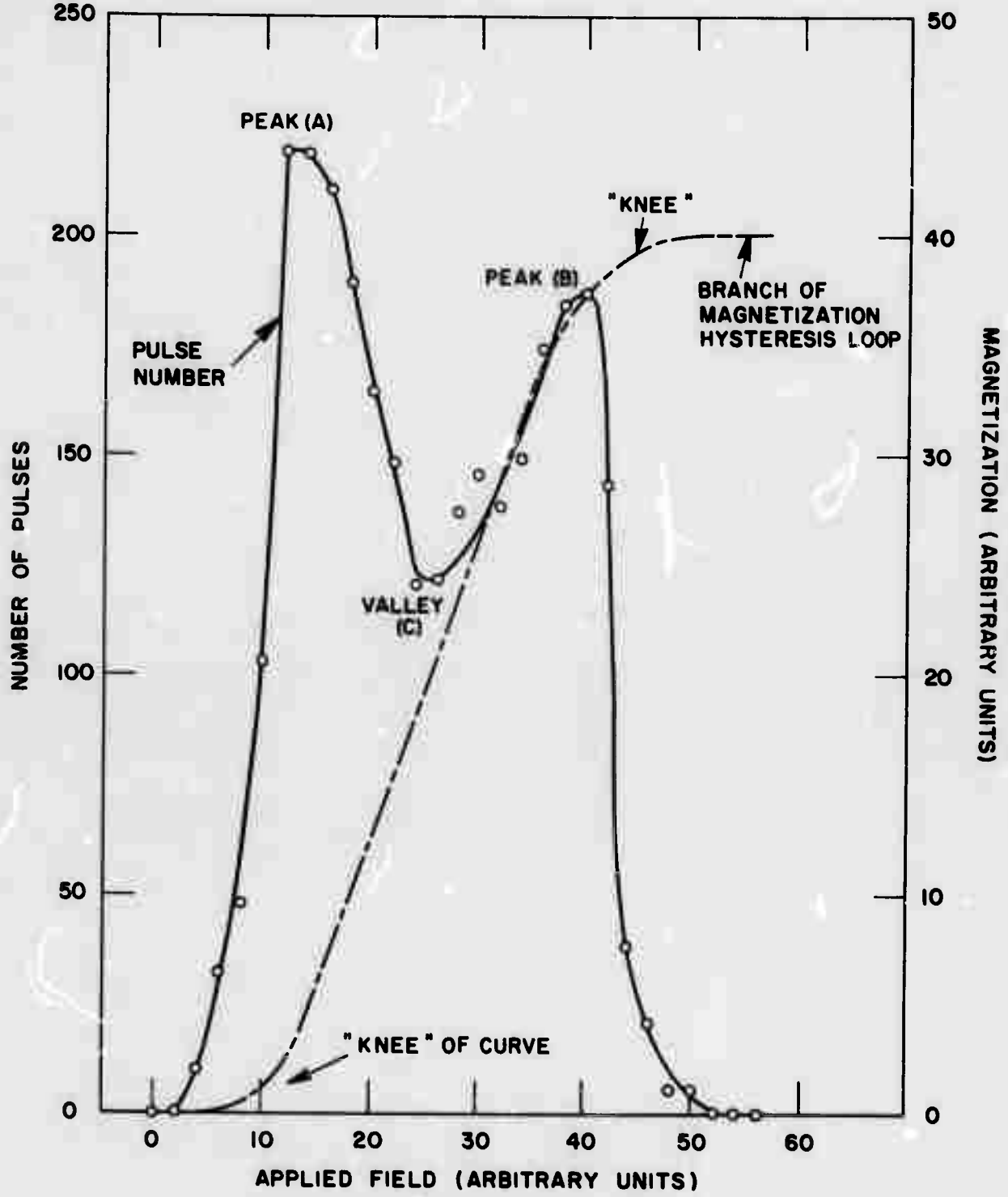


2301

FIGURE 10. MULTISCALING BARKHAUSEN PULSE DISTRIBUTION FOR ANNEALED POLYCRYSTALLINE Fe-3.2%Si SPECIMEN

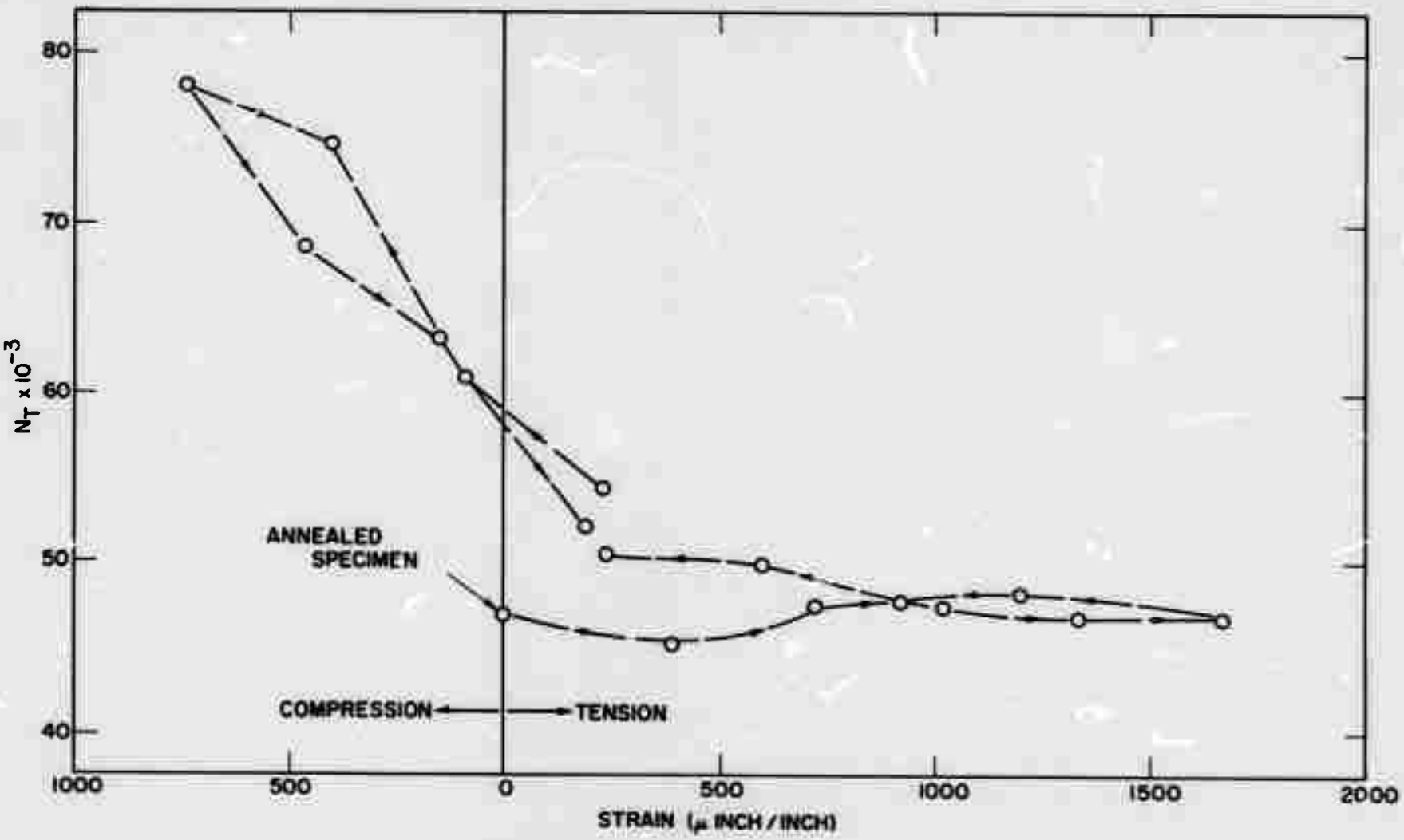


FIGURE 11. TOTAL BARKHAUSEN COUNT NUMBER VERSUS ELASTIC STRAIN FOR POLYCRYSTALLINE Fe-3 2%Si

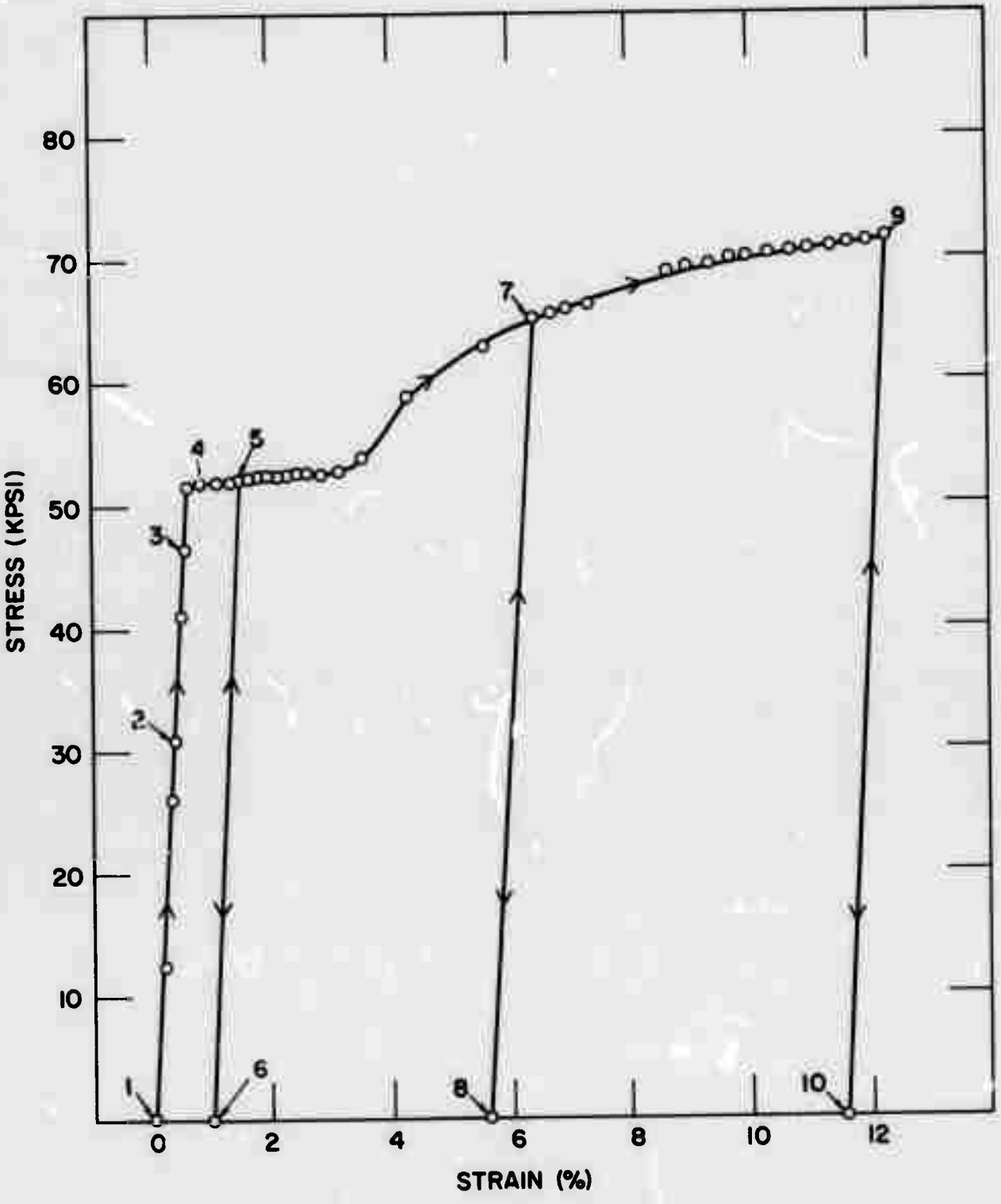


FIGURE 12. STRESS-STRAIN CURVE FOR POLYCRYSTALLINE Fe-3.2%Si SPECIMEN

Figure 13 shows the dependence of the total count number per magnetization reversal, $N_T$, as a function of tensile strain. $N_T$ increases markedly as the specimen is plastically elongated. Once the specimen is initially plastically strained, $N_T$ is less for the loaded condition as compared to the unloaded condition. However, for the annealed condition, $N_T$ is, within experimental error, independent of elastic strain. The latter result is peculiar to the well annealed initial state of the specimen; as shown by the figure, after initial yielding of the material, subsequent application of load within the elastic range produced pronounced changes in $N_T$.

Figure 14 shows how $\langle h \rangle$ was found to vary with elastic and plastic strain. In the elastic range (points 1-3 in Figure 12), $\langle h \rangle$ decreased slightly. Furthermore, after initial yielding, $\langle h \rangle$ is always increased by lowering the stress below the (current) yield stress, and vice versa. The behavior of $\langle h \rangle$ and $N_T$ for the plastically deformed specimen as the specimen was first unloaded and then elastically reloaded (for example, between 7 and 8 in Figures 13 and 14) was determined in detail. Figures 15 and 16 show representative results for $\langle h \rangle$ and $N_T$ respectively. As the graphs reveal, both parameters increased markedly and linearly with elastic recovery upon unloading, and, upon elastic reloading, decreased along the original curve. Thus it is clear that (1) the behavior of $N_T$ and $\langle h \rangle$ for a specimen which has been plastically deformed differs somewhat from their behavior for an annealed specimen; (2) increased plastic deformation increases both $N_T$ and $\langle h \rangle$; (3) $N_T$ and $\langle h \rangle$ vary strongly and approximately linearly with elastic strain of a previously plastically deformed specimen.

Figure 17 shows the multiscaling pulse distributions (as displayed by a cathode ray oscilloscope) for each of the selected stress-strain states identified by arrows in Figure 12. The significance attributed to the changes in these distributions will be discussed shortly.

### 3.1.3 Results for the Single Crystal Specimen

Pulse height distributions and multiscaling distributions were also obtained using a rectangular single crystal specimen of Fe-3.1%Si, the principal face of which is parallel to the (100) crystalline plane. The dimensions and crystallographic orientation are shown in Figures 18 and 19. Available fixturing permitted only compressive loads to be applied to this specimen; because of its value, it was not plastically deformed. Figure 20 shows pulse height distributions for the crystal in its annealed unstressed state, and for an applied compressive stress of 6.1 kg/mm$^2$ (8100 psi). The nonlinear character of the logarithmic plot is apparent. The shape of the distribution is not appreciably affected by the application of the load;

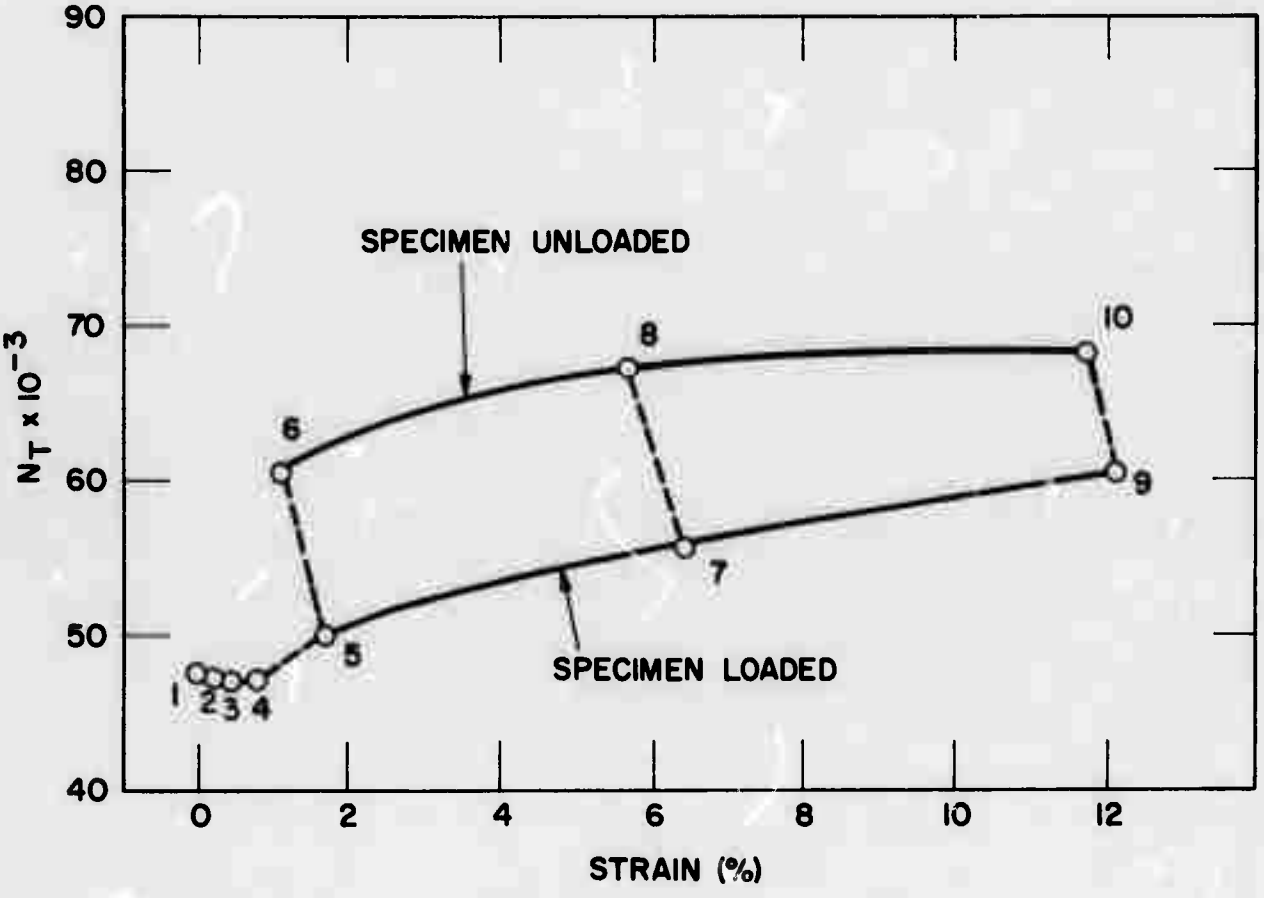


FIGURE 13. TOTAL BARKHAUSEN PULSES PER MAGNETIZATION REVERSAL VERSUS STRAIN

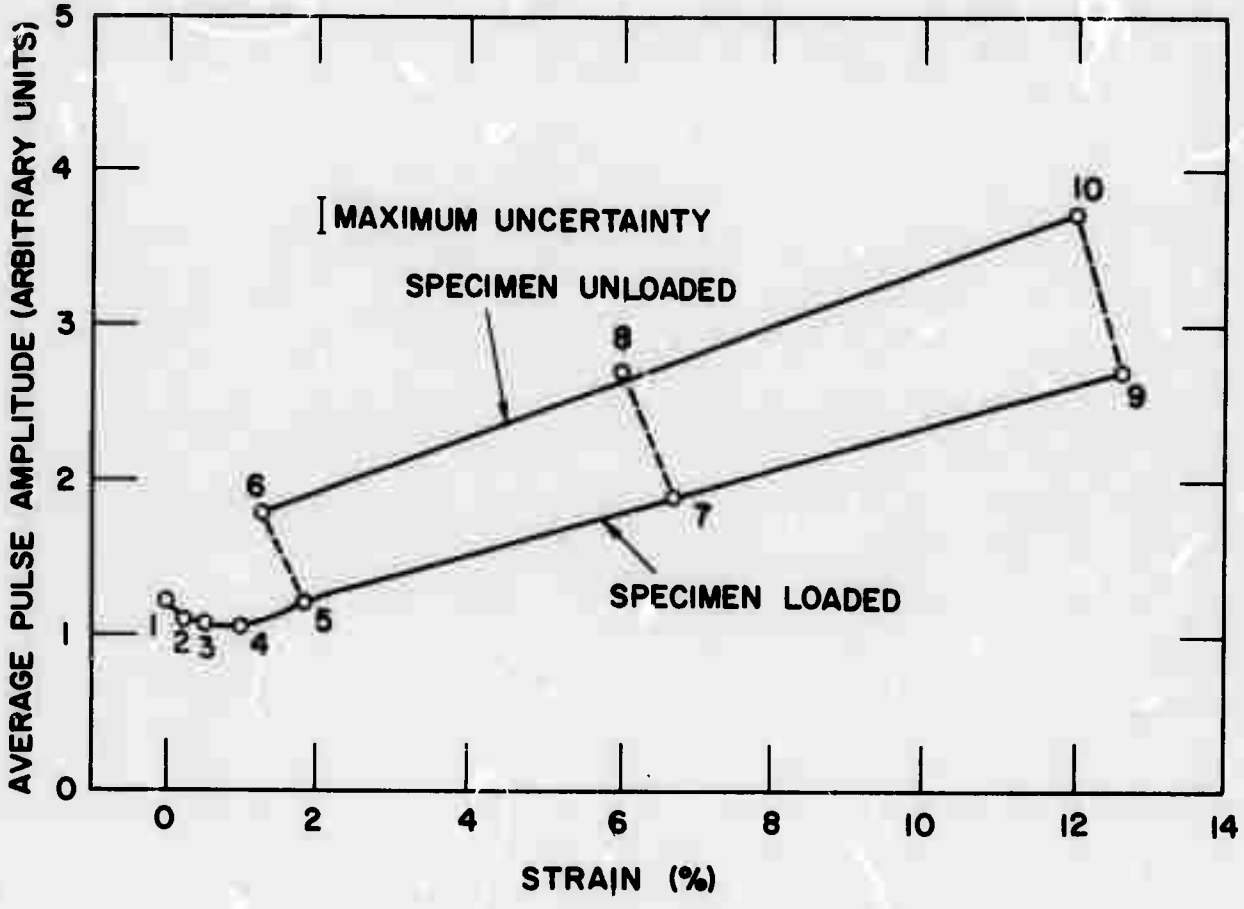


FIGURE 14. AVERAGE BARKHAUSEN PULSE HEIGHT VERSUS STRAIN

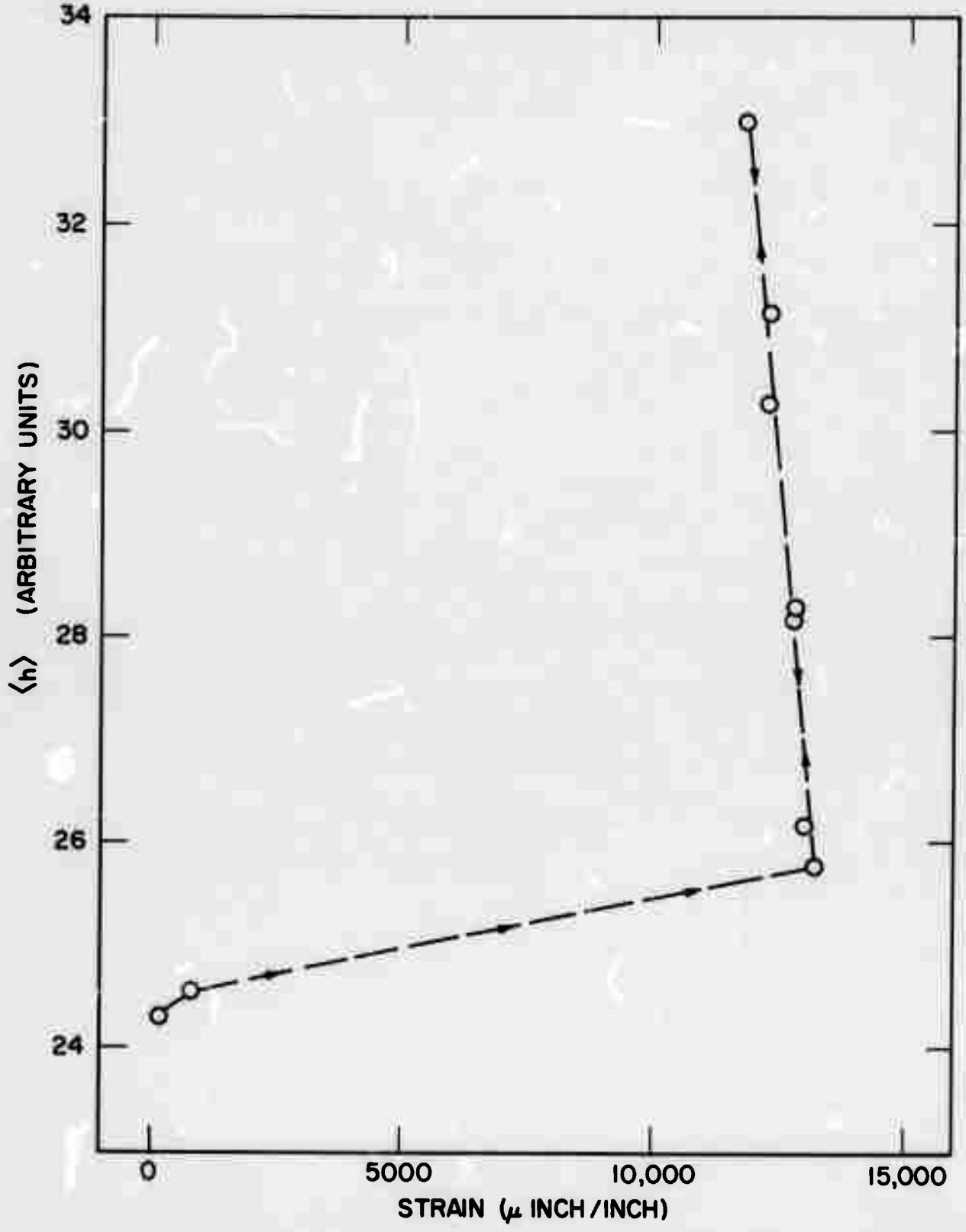


FIGURE 15. VARIATION OF AVERAGE PULSE HEIGHT WITH ELASTIC RECOVERY AND RELOADING OF A PLASTICALLY DEFORMED SPECIMEN

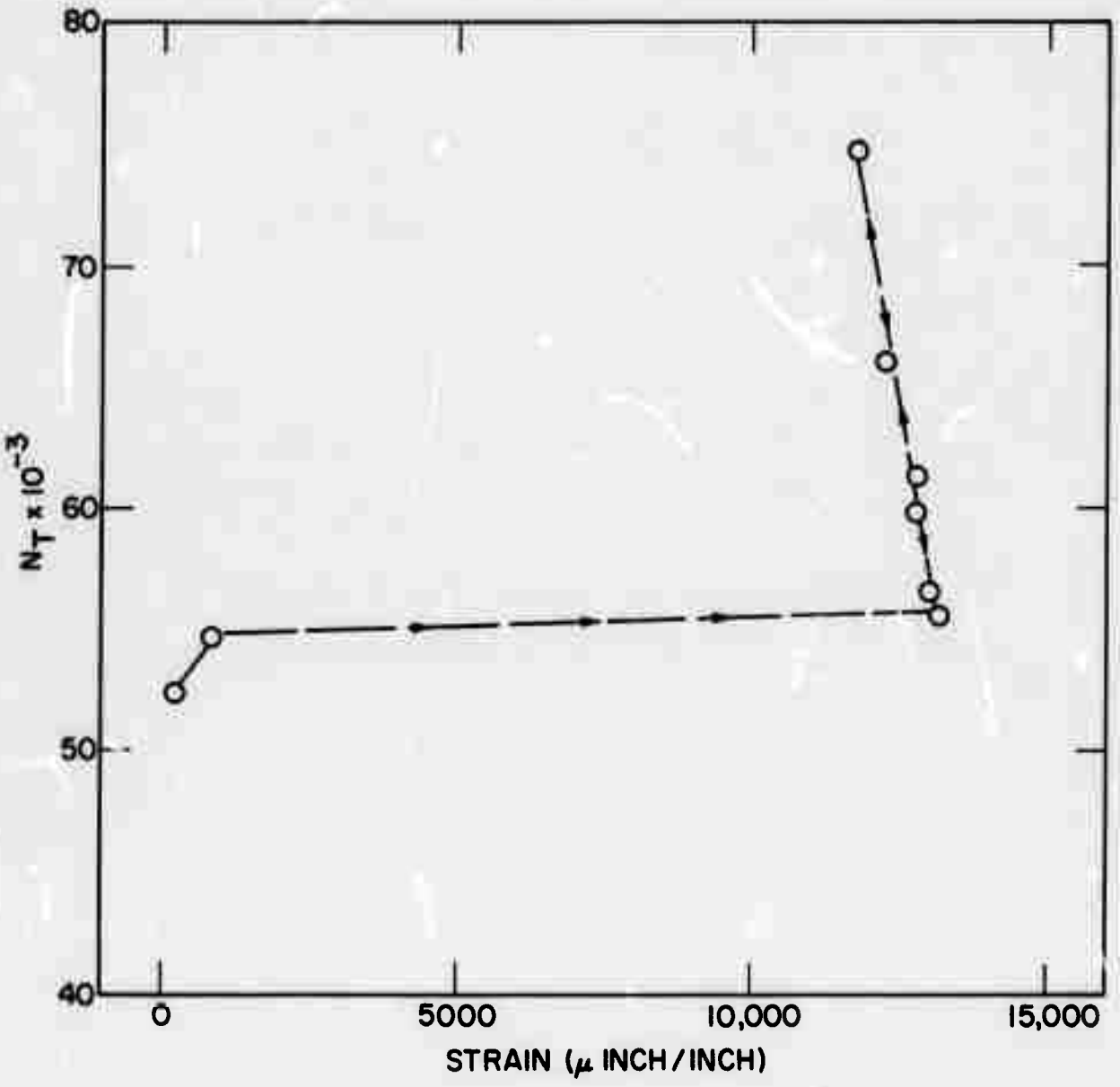


FIGURE 16. VARIATION OF TOTAL COUNT NUMBER WITH ELASTIC RECOVERY AND RELOADING OF A PLASTICALLY DEFORMED SPECIMEN

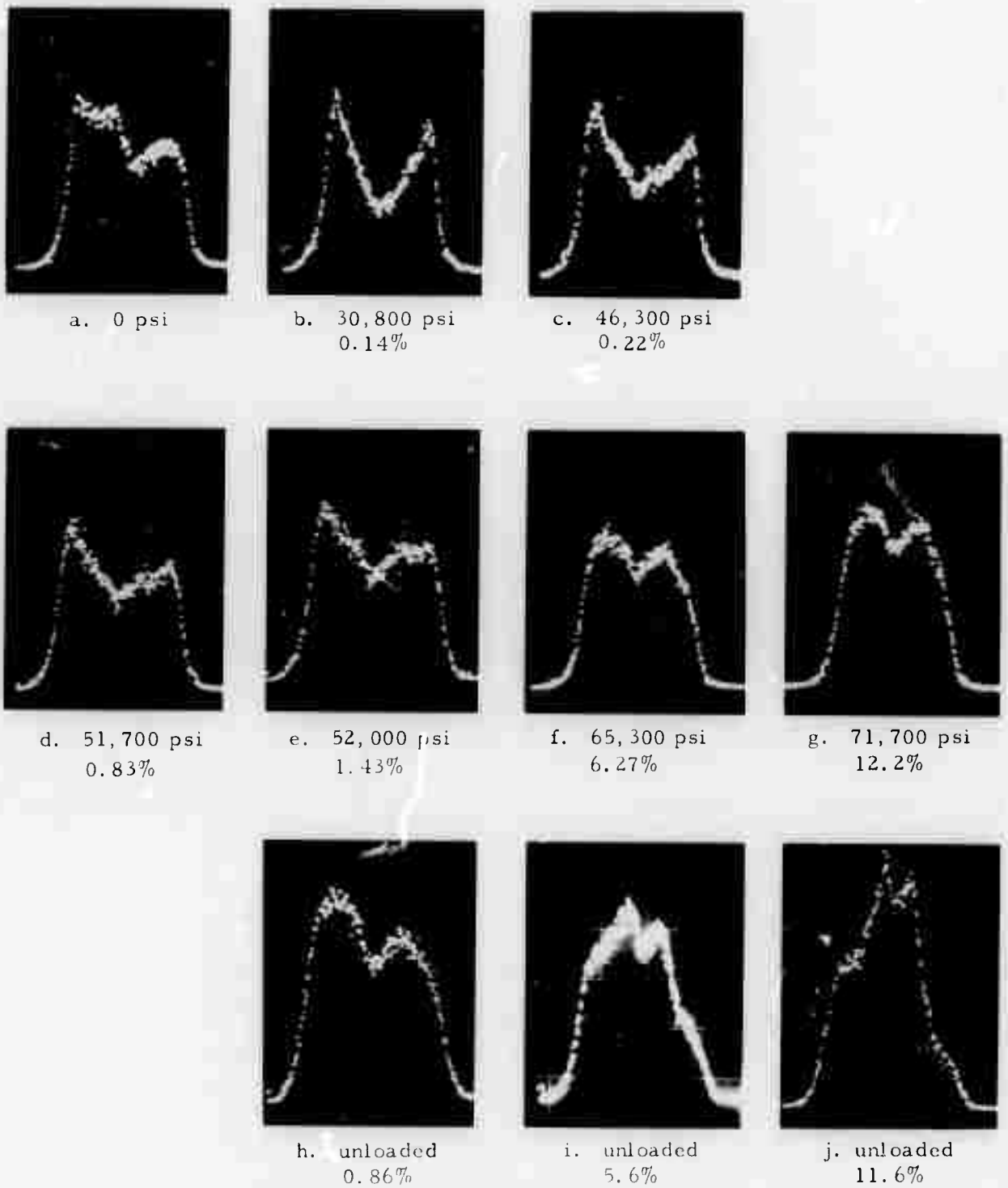

a. 0 psi
b. 30,800 psi 0.14%
c. 46,300 psi 0.22%
d. 51,700 psi 0.83%
e. 52,000 psi 1.43%
f. 65,300 psi 6.27%
g. 71,700 psi 12.2%
h. unloaded 0.86%
i. unloaded 5.6%
j. unloaded 11.6%

FIGURE 17. MULTISCALING BARKHAUSEN PULSE DISTRIBUTIONS FOR VARIOUS STRESS-STRAIN STATES (POLYCRYSTALLINE Fe-3.2%Si)

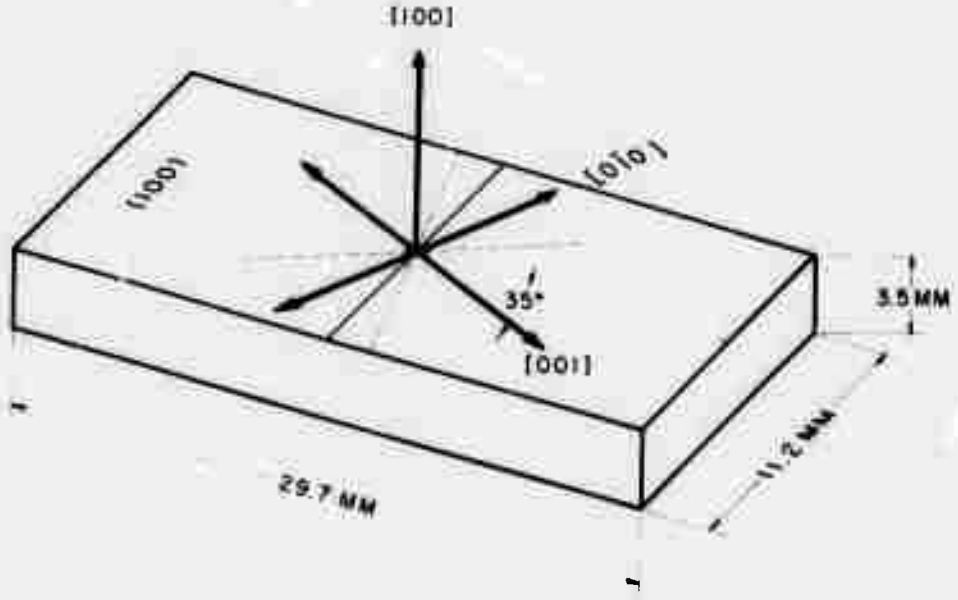


FIGURE 18. DIMENSIONS AND CRYSTALLOGRAPHIC ORIENTATION OF Fe-3.1%Si SINGLE CRYSTAL

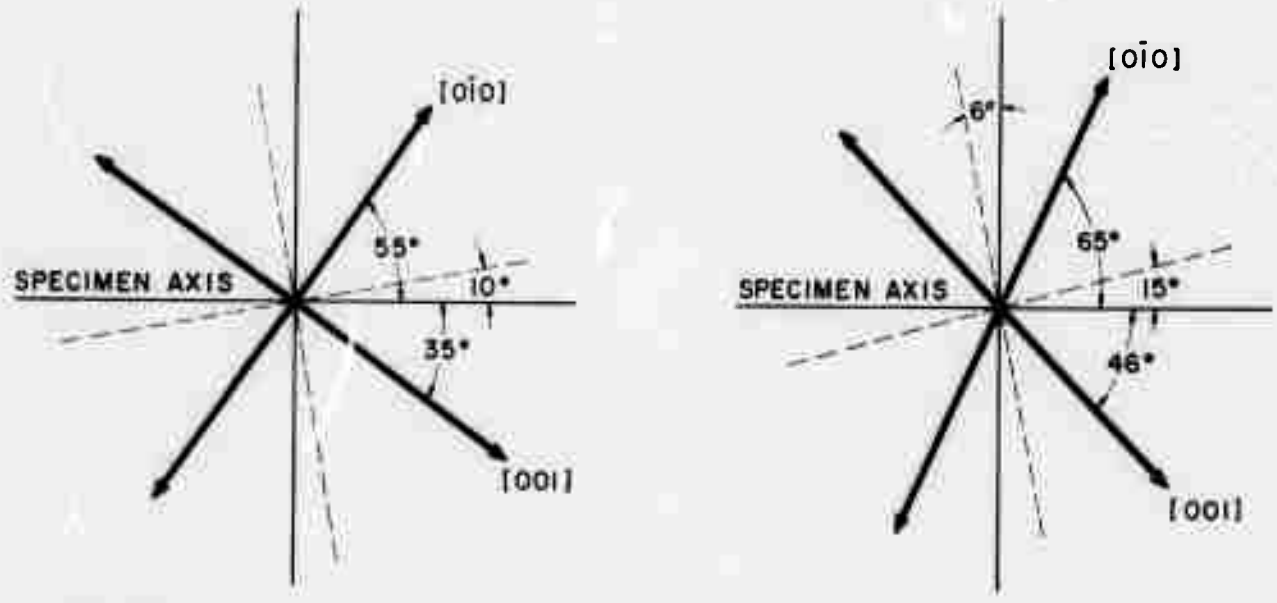


FIGURE 19. ORIENTATION OF CRYSTALLINE AXES RELATIVE TO MAGNETOOPTIC VIEWING PLANE

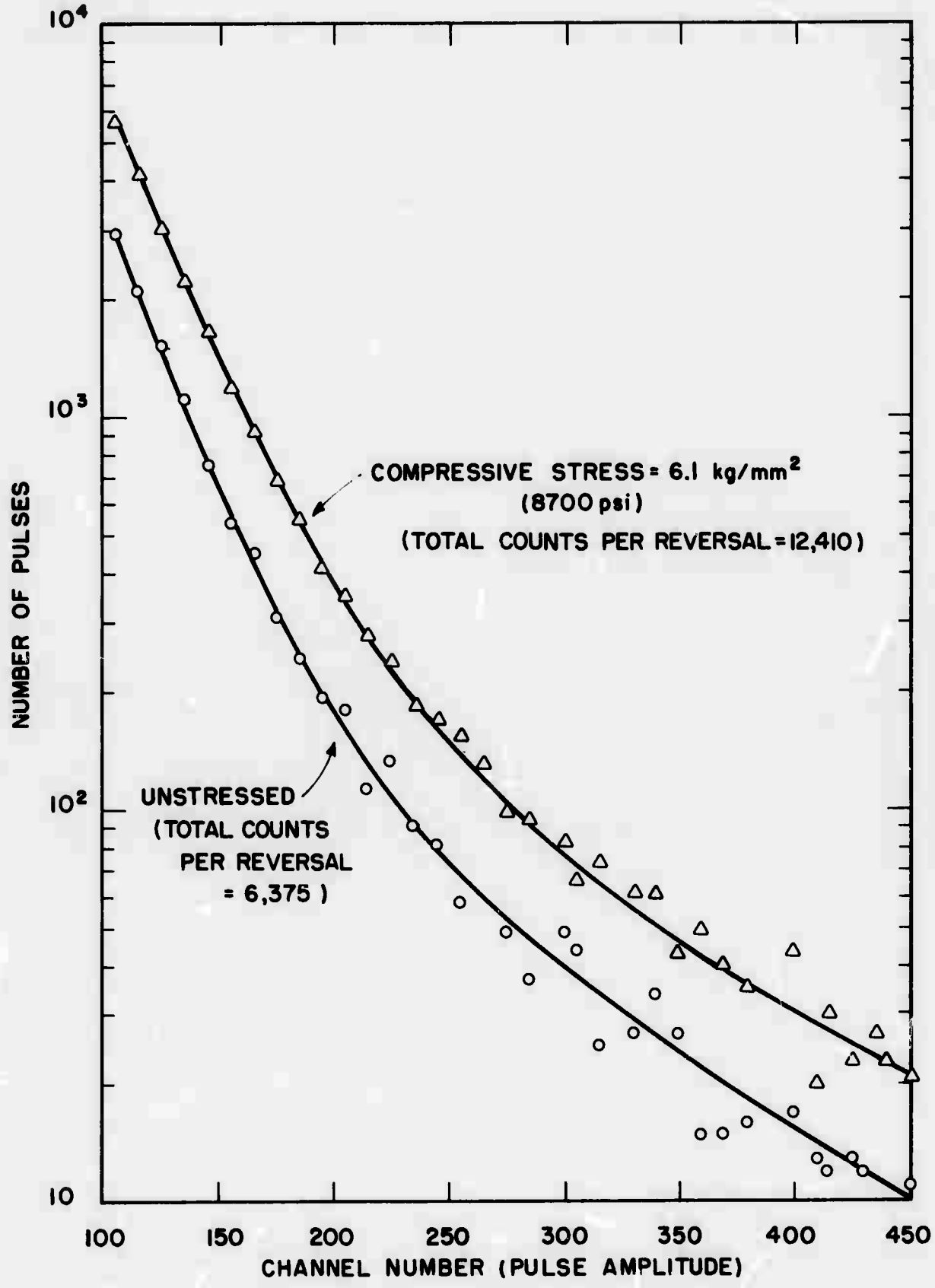


2299

FIGURE 20. BARKHAUSEN PULSE HEIGHT DISTRIBUTIONS FOR Fe-3.1%Si SINGLE CRYSTAL

however, the total number of pulses per magnetization reversal is nearly doubled by applying the load. This is a much greater increase in count number than for a corresponding compressive load on the polycrystalline specimen, indicative of the important role played by crystallographic orientation in the influence of stress on the Barkhausen effect.

The multiscaling pulse number distributions corresponding to the unloaded and loaded conditions of the single crystal are shown in Figure 21. The complex structure of the multiscaling distribution for the unloaded crystal, on close inspection is seen to comprise two prominent peaks, one somewhat broader than the other. As is apparent on examining the result for the loaded specimen, the increase in total count number is due primarily to a large increase in counts near the center of the magnetization reversal.

## 3.2 Magnetooptic Cinematography

Utilizing the Kerr magnetooptic effect, studies were made of the magnetic domain structure on a (100) surface of the Fe-3.1%Si single crystal. Figure 22 shows a still photograph of the domain structure for the unloaded crystal in its nominally demagnetized state; the inferred directions of magnetization are indicated by arrows drawn on the photograph. The characteristic V-shaped structure is formed by domains separated by 180° Bloch walls which run parallel to the [010]-direction and the [001]-direction in the crystal; these are, of course, magnetically easy axes in iron. (Consult the crystallographic orientation illustrated in Figure 19). The "checkerboard" arrangement is produced by additional 90° Bloch walls which run parallel to the intermediate [011]-type directions. A more detailed description of static domain photographs is given in the Phase II Final Report.

High speed (5000 frames/sec) cinematographic studies were made of the single crystal domain dynamics during a magnetization reversal as a function of applied compressive stress. Figure 23 shows selected frames from these films for zero load and at 7000 psi compressive stress. Because of the optical arrangement used in the high speed cinematographic experiments only the central portion of the specimen is viewed as can be seen on comparing Figure 23 to the statically obtained photograph in Figure 22 where the entire specimen face is viewed. Examination of the movie results show that for the unloaded specimen, although the magnetization reversal proceeds primarily by movement of 180° walls, the 90° walls still play an important role, especially in the "knee" regions of the magnetization curve where magnetization is found to proceed by gross rearrangements of domains involving both 180° and 90° walls. By contrast, virtually

a. Unloaded

b. Compressive Stress = 8100 psi

FIGURE 21. MULTISCALING BARKHAUSEN PULSE DISTRIBUTIONS FOR Fe-3.1%Si SINGLE CRYSTAL

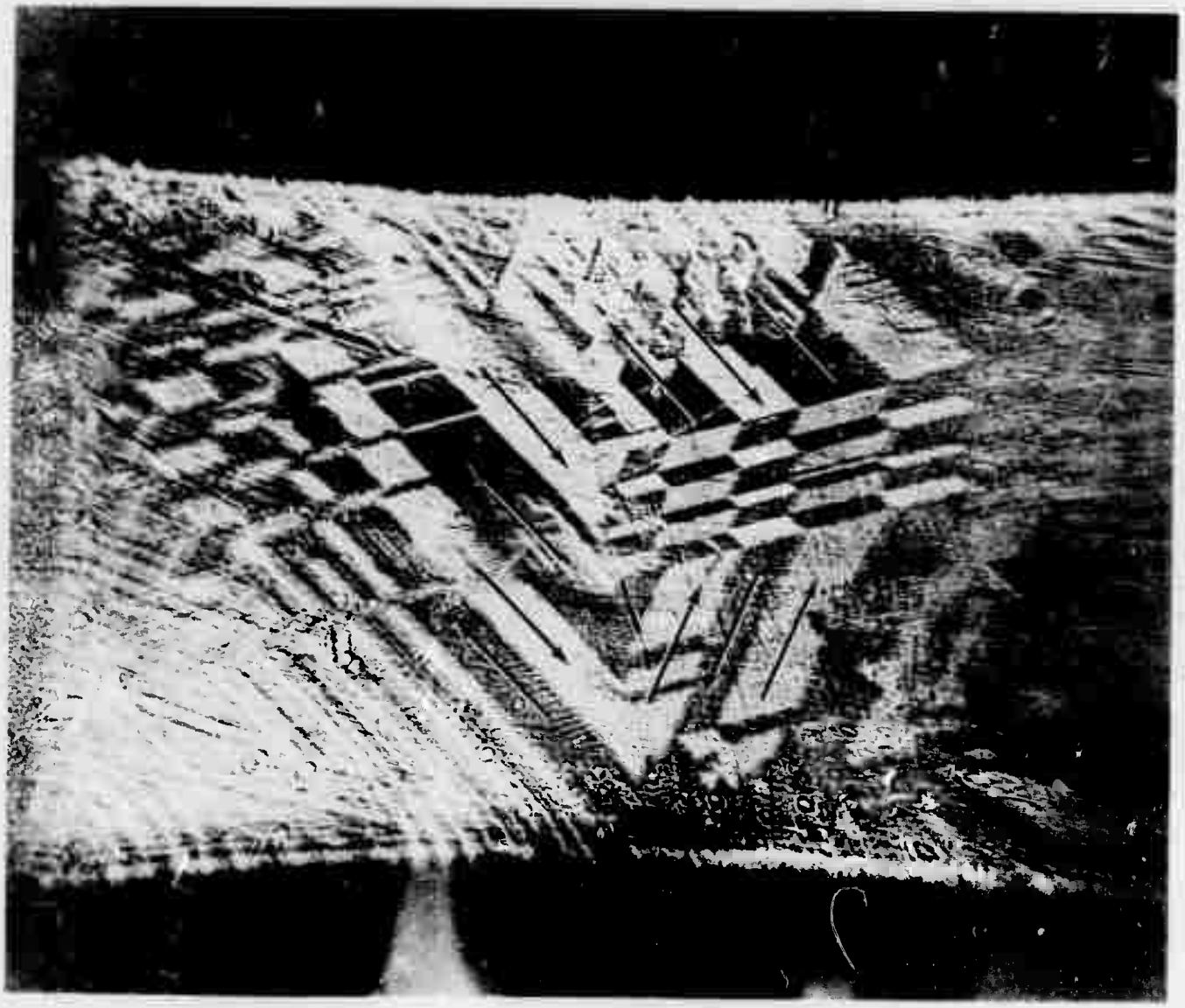

FIGURE 22. OVERALL DOMAIN STRUCTURE OF DEMAGNETIZED Fe-3.1%Si SINGLE CRYSTAL

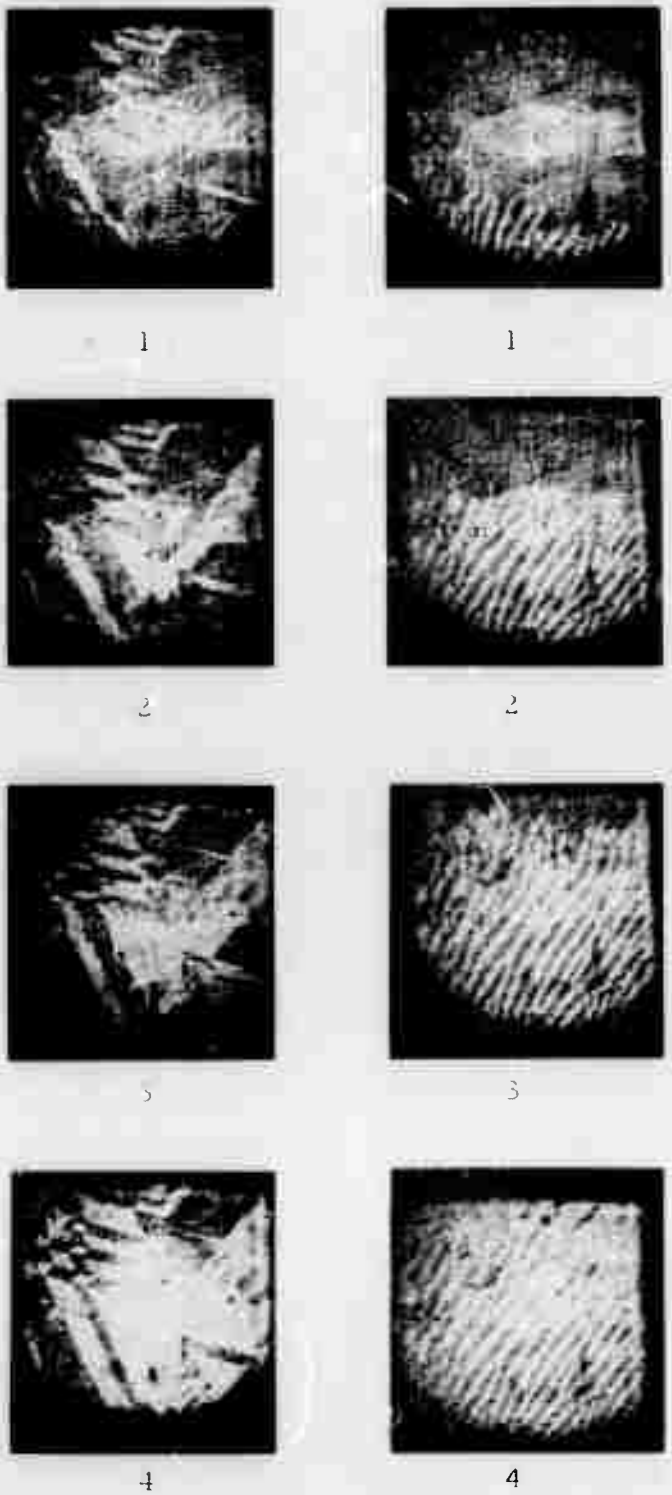


Original framing rate: 5000/sec

Interval between successive frames shown here: 1/20 sec

Magnification: 3X

a. Crystal Unstressed b. 6.6 kpsi Uniaxial Compression

FIGURE 23. SINGLE CRYSTAL DOMAIN STRUCTURE AT VARIOUS STAGES OF MAGNETIZATION REVERSAL

no 90° walls are apparent during the magnetization reversal under applied stress (Figure 23, e, f, g and h).

A full analysis of these extraordinary films will require considerable time to complete. Even now, however, they have suggested and support an important tentative theoretical model which helps to explain several features of the inductive search coil results; this is elaborated in the ensuing section.

## 4. DISCUSSION OF RESULTS

The foregoing data permit several tentative inferences regarding the basic mechanisms involved in the Barkhausen effect. First, there is the matter of how the rate of occurrence of Barkhausen jumps is distributed with respect to the technical magnetization curve. Figure 10, page 20, shows that for the annealed, unstressed polycrystalline specimen, Barkhausen jumps of the amplitudes detected occur at the greatest rate on the "knees" of the magnetization curve. An examination of the complete magneto-optic film of the single crystal further suggests that, in the unstressed state, large, complex domain rearrangements, involving 90° Bloch walls, are associated with the knees of the magnetization curve, whereas the steep, central portion corresponds predominantly to shifting of 180° Bloch walls. Moreover, the application of stress tends to suppress the 90° wall structures. In combination, these two results suggest that the peaks of the multiscaling distributions are indicative of 90° wall rearrangements, and should be less prominent, compared with the central part of the distribution, for a stressed condition as compared to an unstressed condition. An examination of the multiscaling distributions for the various stress-strain states of the polycrystalline specimen (Figure 17) reveals only one apparent exception to this, namely, the case for 0.14% (elastic) strain (Figure 17). Since this corresponds to the first application of load to an annealed specimen, the apparent anomaly is probably due to initial microstrain hardening which is known to occur in silicon iron at an approximately equivalent strain.[9]

The multiscaling distributions for the Fe-3.1%Si single crystal, shown in Figure 21, page 32 provide further evidence in regard to the effect of stress on domain dynamics. The distribution for the unloaded crystal (Figure 21a), though of somewhat complex structure, does show the characteristic peaks in the location of the knees of the magnetization curve; a central peak is also present. Under compressive stress, the peaks on either side of the central region essentially vanish, and the central peak grows somewhat in amplitude. In accordance with the previously mentioned hypothesis, this bears the interpretation that the Barkhausen jumps associated with the 90° Bloch wall structure have been largely eliminated, while Barkhausen jumps associated with the 180° wall structure are not only preserved, but accentuated.

A further peice of evidence consistent with the hypothesis concerning the multiscaling distribution is the analog Barkhausen signature shown in Figure 24. Although this analog signature cannot be rigorously compared to a multiscaling distribution, the two do have a feature in common, namely,

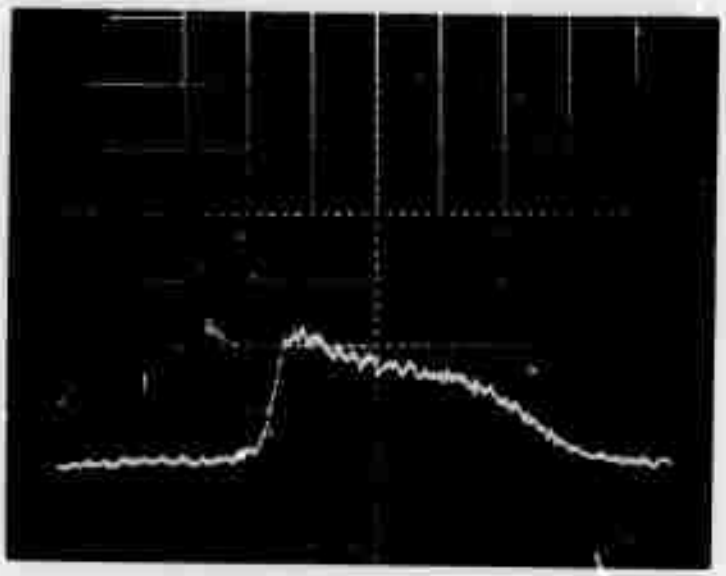

a. Ring-half not subjected to thrust load (original compressive stress condition)

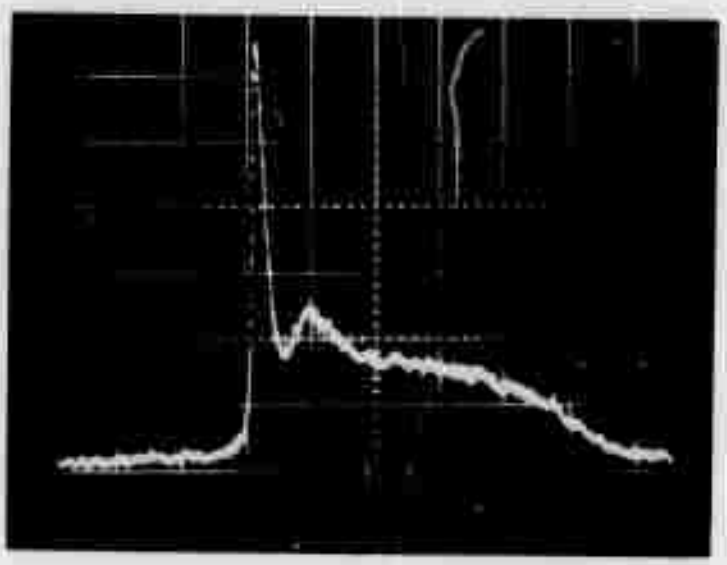

b. Ring-half subjected to thrust load (original compressive stress partially relieved)

FIGURE 24. ANALOG BARKHAUSEN SIGNALS FOR TWO COMPONENTS OF SPLIT INNER RING THRUST BEARING (AISI 52100 STEEL)

each indicates how the "strength" of the Barkhausen jump activity is distributed with respect to the technical magnetization curve. Figures 24a and 24b are the analog signatures of, respectively, the normally unloaded and normally loaded halves of a split inner ring of a jet engine main shaft bearing. In its original condition, the raceway of these rings is in a high residual compressive stress, deliberately induced to improve fatigue resistance. The signature of the ring half which experienced the service thrust load shows a pronounced peak at a location in the distribution which corresponds to a magnetization curve "knee". The signature of the opposing ring half shows no such peak; in fact, the signature is essentially identical to that of a similar component which has not been used. Thus, the development of the peak in the analog Barkhausen signature may be interpreted to reflect a loss of beneficial residual compressive stress.

The aforementioned hypothesis may also account for the departure of the logarithmic pulse height distribution from linearity, especially evident for the single crystal specimen (Figure 20), but also present, though less pronounced, in the distributions for the polycrystalline specimen. The general curvature of these graphs suggests that they may represent two distinct pulse populations with somewhat different logarithmic slopes. It is plausible that the "small pulse" population principally reflects Barkhausen jumps accompanying the motion of 180° domain walls, while the "large pulse" population principally reflects jumps due to large-scale domain rearrangements involving 90° walls.

Thus this investigation suggests the following general picture of how stress affects the production of Barkhausen jumps. First, Barkhausen jumps are of two basic types: one, predominantly large jumps which occur as large-scale rearrangements of complex domain structures; and two, predominantly smaller jumps which occur in connection with the movement of 180° Bloch walls, and which therefore occur mainly along the steepest part of the magnetization curve. Secondly, in the presence of a mechanical stress, a domain structure consisting of parallel domains separated by 180° Bloch walls is energetically preferred, and complex domain structures with which the larger Barkhausen jumps are associated are suppressed. Thus the average jump size is, in general, diminished by the application of stress.

Plastic deformation greatly increases the dislocation density in a specimen, and it is to be expected that this should increase the number of Barkhausen jumps which occur during a magnetization reversal; this is

borne out by the data shown graphically in Figure 13. As shown in Figure 14, the average inductive pulse amplitude also increases with the extent of plastic deformation, but, at a given deformation, is greater for the unloaded as compared to the loaded condition.

## 5. CONCLUSIONS AND RECOMMENDATIONS

The most important basic inference to be drawn from the data presented here is that of the "two populations" model of Barkhausen jumps, that is, one population of jumps associated with abrupt rearrangements of complex domain structures involving both 180° and 90° Bloch walls, and a second population of characteristically smaller jumps associated with impediments to the motion of 180° walls. Although this model must be regarded as tentative subject to further investigation, it does appear to account for both the magnetooptic and inductive pulse height results reported here. Moreover, it provides an important basis for understanding certain features of the behavior of the existing Barkhausen effect instrumentation for stress measurement, and for rationally improving its design. It is known, for example, that for most steels, the response of the instrument tends to "flatten out" at values of tensile stress somewhat below the yield stress. This may be associated with the suppression of the larger, gross rearrangements of domain structure. This suggests that an instrument tailored to indicate the frequency of occurrence of "small" jumps relative to "large" jumps may be more sensitive at higher stress values than one which simply measures something proportional to the total number of jumps without regard to relative magnitudes. Such a design approach, being based on ratios rather than absolute values, may also reduce the sensitivity of the instrument to probe lift-off effects. Since the rate of occurrence of the smaller jumps associated with 180° wall movement are expected to be governed strongly by the density of lattice imperfections, it may also be possible to distinguish such effects from those governed by macroscopic stress distributions.

Taking a longer range (and therefore more speculative) view, the capabilities of the multichannel pulse height analyzer for rapid accumulation, sorting, and presentation of digital information derived from the Barkhausen signal may be extended to provide an essentially real time multiparameter analysis of the signal to yield simultaneously not only the stress but other metallurgical parameters which influence the Barkhausen effect as well.

It is, of course, evident that much further work with the pulse analysis approach to studying the Barkhausen effect and the conditions which influence it is needed. The limited results discussed here are merely indicative of the potential value of the approach in nondestructively characterizing the metallurgical state of ferromagnetic components. Several avenues of future work with the method are apparent. Clearly, the range of specimen materials needs to be extended to include successively the mild carbon steels and the more complex alloy steels. A study

of effects of grain size and preferential orientation is needed; commercially available nuclear pulse instrumentation modules are available for this. With this refinement, a definitive test of the previously mentioned hypothesis regarding the distinguishability of 90° wall jumps and 180° wall jumps could possibly be made. Further study of other pulse characteristics, including duration, impulse, and temporal correlation may also be valuable, especially in discriminating among pulses associated with Barkhausen jumps occurring at various depths within the specimen.

Further studies with the magnetooptic cinematography method may be expected to clarify the effects of grain size and orientation, material composition, plastic deformation, and macroscopic stress distributions.

# REFERENCES


1. Barkhausen, H., "Zwei mit Hilfe der neuen Verstarker entdeckte Erscheinungen," Physik. Z. 20, 401-043 (1919).

2. Bloch, R. J., "Application of Portable Magnetic Equipment to the Nondestructive Determination of Stress in Ferromagnetic Material," Presented at Symposium on Advanced Nondestructive Testing Techniques, Army Materials and Mechanics Research Center, Watertown, Mass., 1-3 June 1971. To be published in Int. J. Nondestructive Testing.

3. Leep, R. W., and Pasley, R. L., "Method and System for Investigating the Stress Conditioning of Magnetic Materials," U. S. Letters Patent 3,427,872 (1969).

4. Donaldson, W. L. and Pasley, R. L., "A New Method of Nondestructive Stress Measurement," Proceedings of the Sixth Symposium on Nondestructive Evaluation of Aerospace and Weapons Systems Components and Materials, Western Periodicals Co., Los Angeles, 1967, pp. 563-575.

5. Leep, R. W., "The Barkhausen Effect and its Application in Nondestructive Testing," Proceedings of the Symposium on Physics and Nondestructive Testing, Dayton, Ohio, 1964, Gordon and Breach, New York, 1967, pp. 439-453.

6. Pasley, R. L., "Barkhausen Effect - An Indication of Stress," Materials Evaluation 28, 157 (1970).

7. Fowler, C. A., Jr., and Fryer, E M., "Magnetic Domains by the Longitudinal Kerr Effect," Phys. Rev. 94, 52 (1954).

8. Tebble, R. S., Skidmore, I. C. and Corner, W. D., "The Barkhausen Effect," Proceedings of the Physical Society 63, 739 (1950).

9. Carson, K. R., and Weertman, L., "Dislocation Density in Single Crystals of Silicon-Iron During Low Cycle Fatigue," Transactions of the Metallurgical Society of AIME, 242, 956 (1968).

10. Stierstadt, K., and Pfrenger, E., "Die Temperaturabhangigkeit des magnetischen Barkhausen - Effekts. I," Z. Physik, 179, 182 (1964).

# APPENDIX A

## SHAPING OF BARKHAUSEN PULSES FOR MULTICHANNEL PULSE HEIGHT ANALYSIS

Although multichannel pulse height analyzers have been used previously for quantitative investigations of Barkhausen pulse amplitude distributions,[10] several innovations were introduced during the course of this program. The first one concerns the shape of the induced voltage pulses. In tests with a pulse generator, it was found that the pulse height analyzer is sensitive to the shape of the incoming pulses. For good linear response and proper operation of the internal voltage discriminator, certain requirements as to pulse shape must be fulfilled, namely, risetime = .25 to 5 $\mu$sec; duration = 2 to 3 $\mu$ sec. As can be seen from the bottom photograph in Figure A1, the Barkhausen pulses do not generally fulfill these requirements. In order to obtain appropriately shaped pulses for the pulse height analyzer, it was found convenient to make use of instrumentation ordinarily used in nuclear spectroscopy, namely, a biased amplifier and a strobed pulse stretcher. The biased amplifier is a linear amplifier which amplifies pulses without changing their shape, but which passes only that part of the signal train higher than some selectable amplitude. This instrument provides good discrimination against background noise and allows Barkhausen pulses which exceed the bias level to be amplified sufficiently to make maximum use of the pulse height analyzer resolution. The strobed pulse stretcher accepts pulses from the biased amplifier and generates approximately rectangular pulses the amplitude of which corresponds exactly to the amplitude of the incoming pulses. The pulse stretcher also has the important feature of rejecting pulses which overlap to an extent that the true amplitude is ambiguous. Figure A1a shows the rectangular output pulse of the pulse stretcher compared to a simulated Barkhausen pulse; Figure A1b shows a Barkhausen noise trace and the corresponding pulse stretcher output displayed on a dual beam oscilloscope. Figure A2 shows representative Barkhausen pulse height distributions obtained with and without the biased amplifier and the pulse stretcher. The improved definition of the distribution with the use of pulse shaping is apparent.

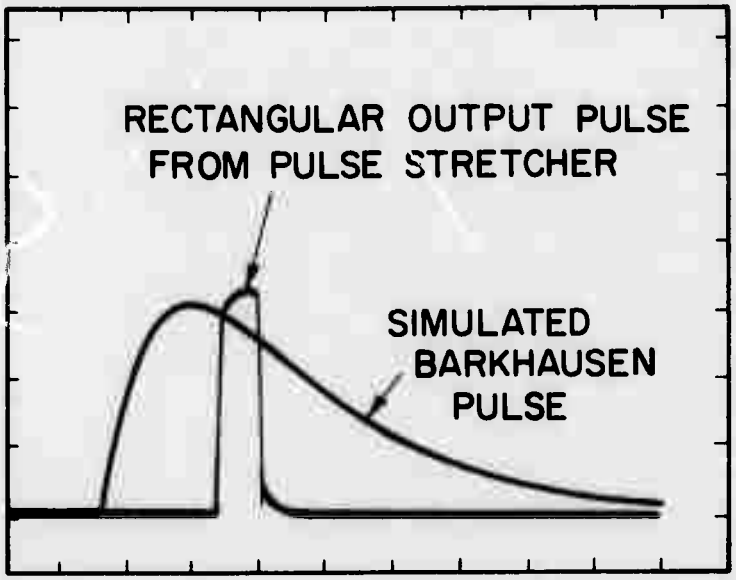


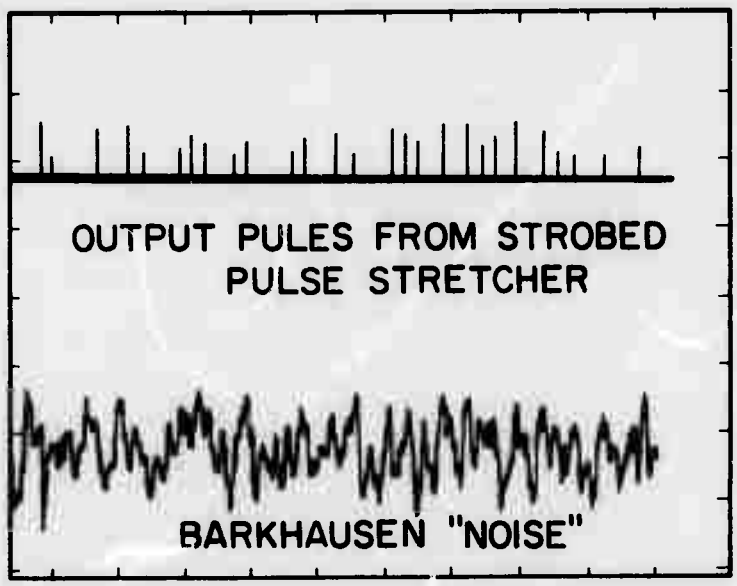


FIGURE A1 PULSE SHAPING EFFECT OF STROBED PULSE STRETCHER

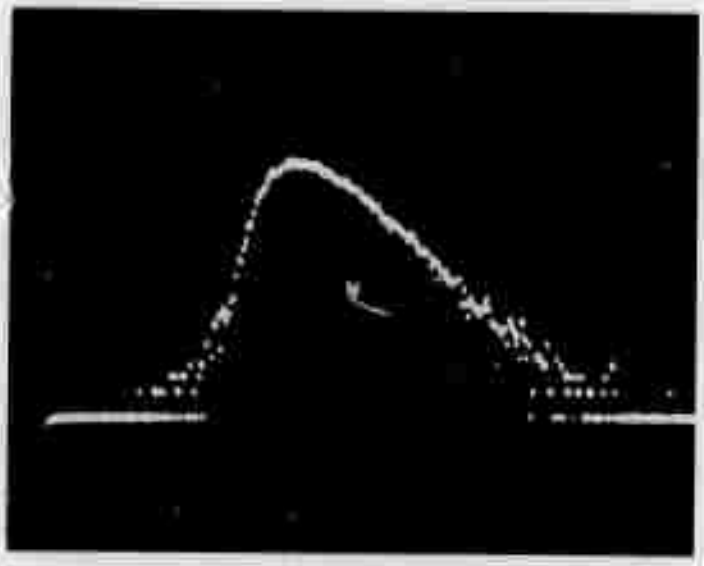

a. Without pulse shaping

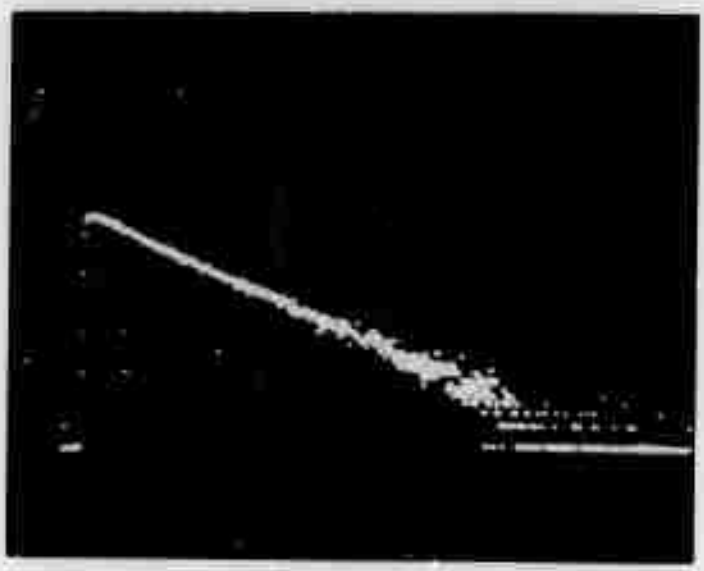

b. With pulse shaping

FIGURE A2. BARKHAUSEN PULSE HEIGHT DISTRIBUTION

# APPENDIX B

## MAGNETOOPTIC PHOTOMETRY

Beside the magnetooptic cinematographic method for the general study of domain dynamics, another approach is to make use of photometric techniques whereby surface magnetization changes are detected by the corresponding changes in intensity of the reflected light beam (see Phase II Final Report for further details). Although in the Phase II Final Report, we reported initial success in detecting Barkhausen jumps photometrically during a magnetization reversal of a Permalloy thin film, the scope and financial resources of the program did not allow us to pursue completely the more difficult problem of detecting the small intensity changes from larger bulk specimens. An approach suggested for enhancing the signal-to-noise ratio in this case is shown schematically in Figure B1. The method depends on achieving image contrast inversion between two channels so that changes in light intensity due to magnetization changes will be in opposite directions. Connecting the two photomultiplier outputs to the two inputs of a differential amplifier results in substantial cancellation of common mode noise. High-pass filtering may then be used to convert abrupt intensity changes into pulses which can be analyzed with a pulse height analyzer. In preliminary work, we have found that splitting the incident beam and providing a separate polarizer and analyzer for each channel enables good contrast inversion to be obtained between the two channels.

This technique appears to be potentially quite useful for the study of magnetization phenomena and if fully developed should prove helpful in interpreting magnetooptic cinematographic observations in terms of Barkhausen activity.

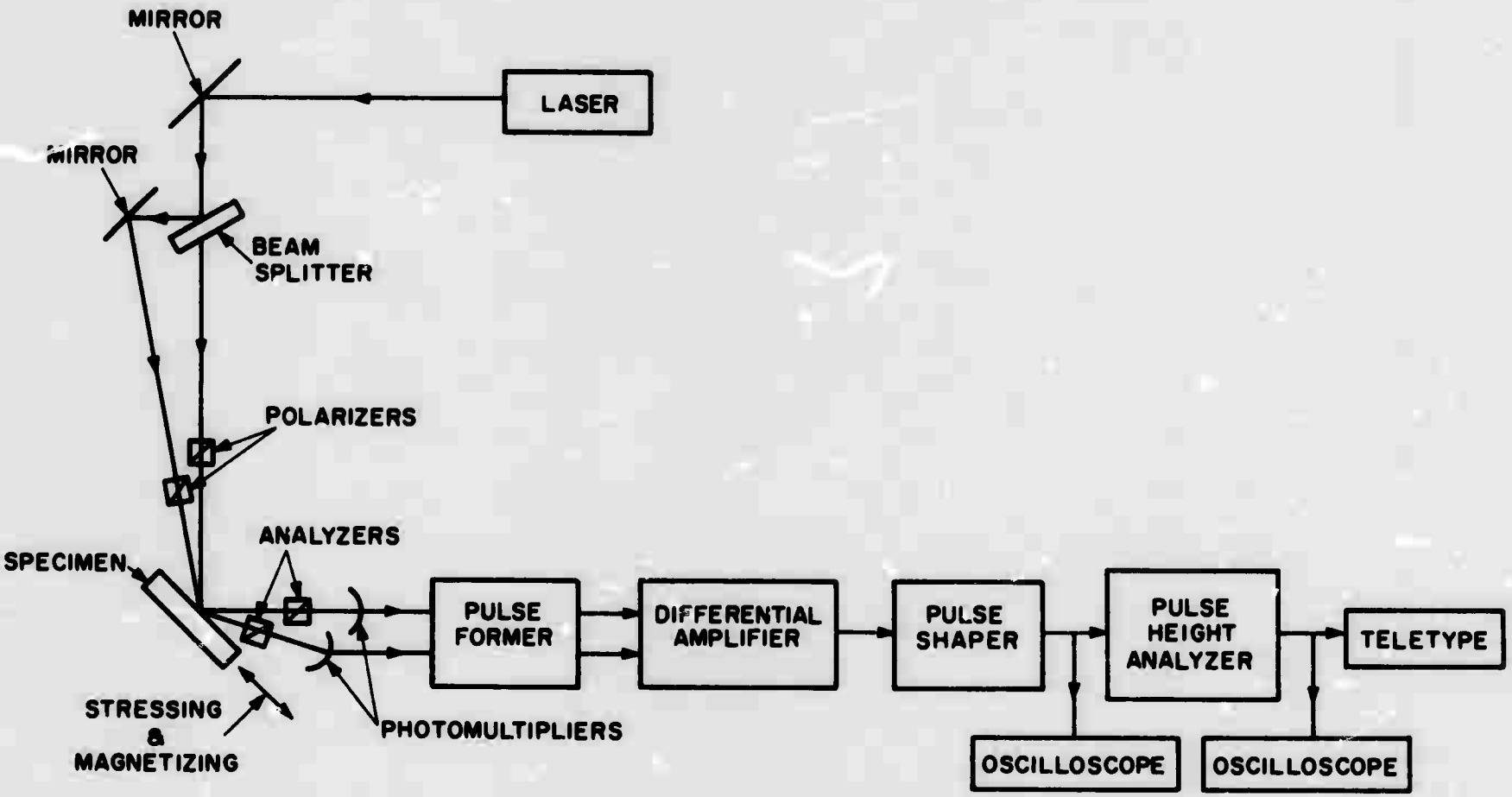


FIGURE B1. SCHEMATIC OF DUAL BEAM MAGNETOOPTIC PHOTOMETRIC BARKHAUSEN EXPERIMENT

# APPENDIX C

## LIST OF PUBLICATIONS AND PRESENTATIONS

"Magneto-Optic Study of Domain Dynamics in a Silicon-Iron Single Crystal," G. A. Matzkanin, C. G. Gardner, D. L. Davidson, presented at the American Physical Society Meeting, Washington, D. C., April, 1970. Abstract published in the Bulletin of the American Physical Society 15, 579 (1970).

"The Influence of Mechanical Stress on Magnetization Processes and Barkhausen Jumps in Ferromagnetic Materials," C. G. Gardner, G. A. Matzkanin and D. L. Davidson, International Journal of Nondestructive Testing (in press, 1971). Presented at the Symposium on Advanced Experimental Techniques in the Mechanics of Materials, San Antonio, Texas, September, 1970.

"Influence of Stress and Plastic Deformation on the Barkhausen Effect in Silicon-Iron", C. G. Gardner, G. A. Matzkanin and J. Lankford, International Journal of Nondestructive Testing (in press, 1971). Presented at the Symposium on Advanced Nondestructive Testing Techniques, Army Materials and Mechanics Research Center, Watertown, Massachusetts, June 1971.

"Barkhausen Jumps in Plastically Deformed Silicon-Iron," C. G. Gardner and G. A. Matzkanin, accepted for presentation at the Seventeenth Annual Conference on Magnetism and Magnetic Materials, Chicago, Illinois, November 1971. To be published in the AIP Conference Proceedings.